Master's Degree Thesis
ISRN: BTH-AMT-EX--2016/D06--SE

Design and Structural Analysis of a Robotic Arm

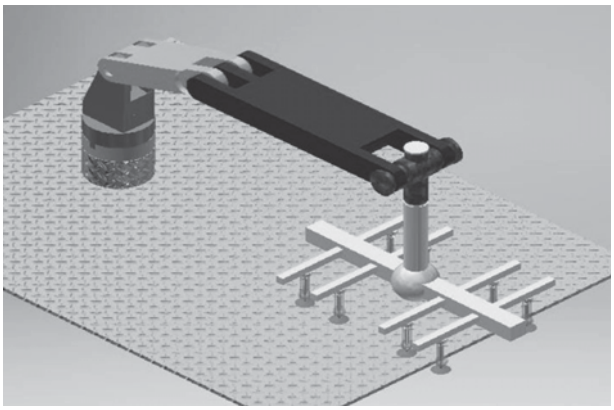

Gurudu Rishank Reddy
Venkata Krishna Prashanth Eranki

Department of Mechanical Engineering
Blekinge Institute of Technology
Karlskrona, Sweden

2016

Supervisors: R.V Jhansi Rao, Signode India Limited (SIG)
Sharon Kao-Walter, BTH

Design and Structural Analysis of a Robotic Arm

Gurudu Rishank Reddy

Venkata Krishna Prashanth Eranki

Department of Mechanical Engineering

Blekinge Institute of Technology

Karlskrona, Sweden

2016

Thesis submitted for completion of Master of Science in Mechanical Engineering with emphasis on Structural Mechanics at the Department of Mechanical Engineering, Blekinge Institute of Technology, Karlskrona, Sweden.

Abstract:

Automation is creating revolution in the present industrial sector, as it reduces manpower and time of production. Our project mainly deals around the shearing operation, were the sheet is picked manually and placed on the belt for shearing which involves risk factor. Our challenge is designing of pick and place operator to carry the sheet from the stack and place it in the shearing machine for the feeding. We have gone through different research papers, articles and had observed the advanced technologies used in other industries for the similar operation. After related study we have achieved the design of a 3-jointed robotic arm were the base is fixed and the remaining joints move in vertical and horizontal directions. The end effector is also designed such that to lift the sheet we use suction cups were the sheet is uplifted with a certain pressure. Here we used Creo-Parametric for design and Autodesk-Inventor 2017 to simulate the designed model.

Keywords:

Autodesk-Inventor 2017, Creo-Parametric, robotic arm, suction cups.

Acknowledgements

This work is carried out at the Department of Mechanical Engineering, Blekinge Institute of Technology (BTH), Karlskrona, Sweden and Signode India Limited (SIG), Rudhraram, India from February 2016 to October 2016 under the supervision of R.V Jhansi Rao.

We wish to express our sincere gratitude to our industrial supervisors, Signode India limited, India for their competent guidance and support throughout the project. We are thankful to our academic and internal supervisor Prof. Sharon Kao-Walter BTH Sweden for her valuable support and advice.

We would also like to express our deepest gratitude to the staff at Signode India limited Mr. Madhu, Mr. Annand and Mr. Prashanth for their timely help, support and everlasting patience. And we would like to thank our beloved Sir. Sravan Kumar from JNTUH Mechanical department for valuable discussions and support. We are thankful to SIG in providing us the required equipment and software to carry out the project.

We are very thankful to our parents for their constant support, love and care.

Karlskrona, October 2016

Gurudu Rishank Reddy

Venkata Krishna Prashanth Eranki

Contents

List of Figures

1 Notation

A	Area
B	Width
D	Diameter of Solid Shaft
E	Young's Modulus
H	Height
I	Moment of Inertia
L	Length
M	Mass
Q	Weight
R	Radial Arm
r	Radius of Solid Shaft
t	Torque acting on Solid Shaft
T	Thickness
V	Volume
W	Load acting on Solid Shaft
$\boldsymbol{\rho}$	Density

Abbreviations

CAD	Computer Aided Design
CFRP	Carbon Fibre Reinforced Plastic
DOF	Degrees of Freedom
FANUC	Fuji Automated Numerical Control
FEA	Finite Element Method
FOS	Factor of Safety
KSI	Kilo pound per Square Inch
SIG	Signode India Limited
RCC	Remote Censor Control

2 Introduction

The most aged methods of metal engaged procedures are shearing and bending. These are the basic operations that are performed for metal working. Shearing is a mechanical operation, cutting of large sheets of metal into smaller pieces of predetermined sizes. When an operation completes an entire perimeter forming a line with closed geometry is known as blanking. Shearing machines are of different types, but a typical shear generally consists of,

- A fixed bed to which one blade is attached.
- A vertically moving crosshead which mounts on the upper blade.
- A series of hold-down pins or feet which holds the material in place while the cutting occurs.
- A gaging system, either front, back or squaring arm, to produce specific work piece sizes.

Shearing operation is generally conducted manually, but it can be conducted using mechanical, pneumatic and hydraulic means also. Currently, the operation is performed manually at the industry but at a very high risk. The raw material is collected by the worker and feeding is done into the shearing machine manually till the sheet is induced completely into it. This operation is very hazardous to the personnel performing the operation. Also, there is a fair chance that automating this process might speed up the rate of work when compared to the manual execution.

To overcome these disadvantages, the entire manual process in the shearing process is to be automated. In this project, a pick and place machine is designed to lift the raw material sheets one by one to the shearing machine. Suction cups are designed as holders for these machines to hold the metal sheets and place it on the conveyor belt of the shearing machine. This auto feeding mechanism will be operated by the sheet guide.

This project undergoes an in-depth study of related topics that are explained in-detail in the future sections. Our main intension is to design this is entire

manually operated system (picking of sheet from stack to feed) into automation, such that it reduces the risk-factor during feeding operation. On developing this system, we reduce the time of action performed that leads to increase in productivity.

2.1 Project Statement

The thesis examines the compelling design of a robotic arm i.e. a pick and place machine and auto feeding mechanism that improves the safety of the workers. The main intension of designing this pick and place machine is there will be no need of manual operation of picking the sheet form stack to shearing machine and the auto feeding mechanism is a continuous process were the productivity could be effected.

2.2 Background Study

This project is discussed mainly on Design and structural analysis of a robotic arm, which reduces the man power and might have a good effect on production rate. This change can motivate the industry and academics such that the business of the firm is increased. The development in automation can reduce the revenue cost and raise in capability of delivering the services at low cost scaling.

To look at the safety of the workmen, we designed a pick and place operator i.e. a robotic arm and for the feeding mechanism two pneumatic cylinders are designed. Earlier we have studied about different feeding mechanisms among those we have designed a new model i.e. using the pneumatic cylinders pushing the sheet forward through the cutting blades [1]. In this process the time of feeding is reduced for each sheet.

We have also studied about RCC control for designing the robotic arm[2]. In this the system integrates manipulator position sensor into the robots control routine. It also gives the robot its ability to interact with nature. So depending upon these conditions the manipulator makes it more efficient by providing self-optimisation system. With this self-awareness of the robot there will be

work safety in the environment onsite. Due to this RCC the efficiency of the manipulator increases. To design these RCC model we need to compare with revolutionary symmetric structure and circular periodic structure, due to this we can achieve low stiffness and material will remain same. We have consulted automation companies like Fanuc Automation Solutions, Rexroth Pneumatic cylinders and many other information sources searching for most reasonable and proper solution.

2.3 Research Problem

In sheet shearing operation, picking of sheet and feeding is undergoing manually which is time taking and risk factor is involved in it. So, for the first phase (picking of sheet from stack) we need to avoid that by using an automotive application i.e. pick and place operator and the auto feeding mechanism is initiated with two cylinders parallel to the sheet. As we have discussed above the pick and placer is regulated as a continuous operation for picking the sheets and placing it on the conveyor belt.

Let us consider the pick and place operator i.e. robotic arm design

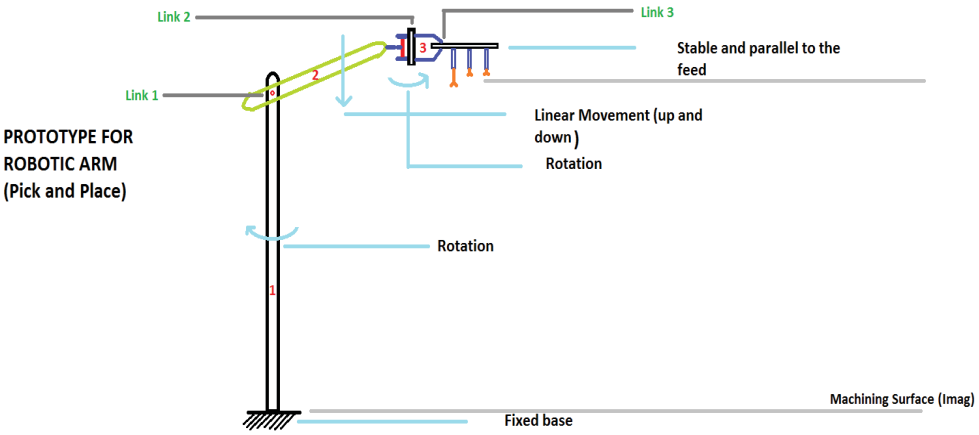

Figure 2.3.1: The Prototype of robotic arm (Pick and Place Operator).

In the above figure 2.3 we need to consider three links of a robotic arm as the base is fixed. These three links are connected to each other by a finge. The link1 is having rotary motion, link 2 is having transient movement upwards and downwards. The link3 is again a rotary motion. Towards the end of link3 an end effector is being placed which is stable and parallel to the feed.

Through this robotic arm, we need to analyse the forces on individual component and the complete arm. Now let us consider the free body diagrams of individual links. The end effector is connected to link3 which is designed with suction cups to lift the sheet. In this we need to analyse the static and dynamic properties of the arm. The pressures at vacuum cups is to be converted to forces and sum of the forces should be greater than the weight of sheet. The pressure and force relations are to be calibrated for each and every link and also for the complete arm.

2.4 Scope of Implementation

The basic idea in this project is implementation of robotic arm. Though it can be implemented in various methods, when different parameters are taken into consideration this model is the most feasible way of implementation. Other ways of enactmenting the model is enabling them to adapt to the surroundings.

2.5 Objectives

- Designing, Modelling and Simulation of the pick and place mechanism. We need to have a time study between currently undergoing manual operation and newly designed automated operation.
- The frequency of this operator, it's repeatability, lifetime etc. are to be found out.
- The choice of the end effector, it's design and analysis should be carried out and documented.

2.6 Research Questions

- How can we automate the process of feeding the metal sheet into the shearing machine?
- How can we design the pick and place robot to meet the requirements of the shearing operation?

2.7 Preliminary Discussion

Before designating about the pick and place operators, we have undergone various methods like use of conveyor belt, pulleys and other simplified mechanisms for this operation. But after a broad search and enquiry, we decided to design an articulated robotic system that makes the entire process more flexible and easier in inducing the mechanism without any employee payload. The reason for selecting only this particular robot as a solution depends upon many factors. The very first one is, these sheets get

painted and printed one by one and stacked at the end of the printing process. The transportation of sheets in this process is done using a frame with suction cups connected to a conveyor belt. The shearing machine is close to the stack and the direction of the feed in the shearing machine is perpendicular to the stack direction. It is complex and complicated or in other words not possible to extend the track of conveyor which is already in use in the printing to deliver the sheet directly into the feed of shearing machine without stacking. It is because the time of one cycle of printing and the time of one cycle of shearing operation of are not same. So, these two process cannot be interlinked without stacking the sheets. Moreover, the space around these two machines is very less to adopt any other automation technique. So, keeping these in mind, we concluded that an articulated robotic arm can do the job of picking and placing in the given space and can correlate these two operations perfectly.

Our main motive is to reduce the risk factor involved physically in this operation. So, we took a forward push of designing a three-jointed robotic system with good and malleable end effector to it. Basically, in our study the articulated robots are of rotary joint system, that can range from two to ten jointed and are mechanized by servo motors. They are various robotic systems, which could be articulated and non-articulated. But according to our operation we prepared rotary joint system which is articulated, in this the space consumption is précised as the joints are supported in chain. The major factors of initiating this system are it is having a continuous path, acceptable degree of freedom, proper grip, cyclic rotation, good accuracy and reach, speed control, repeatability and high resolution.

2.7.1 Articulated Arm Robots

Articulated arm robots are generally used to perform risky, treacherous and highly repetitive and obnoxious works. This entire system is controlled by a trained operator using a portable device like a teach pendant to a robot to do its work manually. The main prospective is not the working of the robot, but how it is to be safeguarded in a regular usage in the industries. The maintenance depends only on technical operators, how hazardous the use of the robot system is its environment conditions, position, initialization requirements, technical errors and other functions.

While many engineers working on these robot systems they could be associated with risks in the operation. In this combination, they need to use safeguarding methods like repetition and backup systems and the entire thing should be monitored by a human operator. As the entire system is to be controlled by an electric device, they are two controllers' servo and non-servo. The use of servo controller gives immense feedback about the robot system and that continually monitors the robot axes which are correlated with the position, velocity and the entire data is stored in the robot's memory. Were as the non-servo controllers do not have the feedback criteria and the system is controlled through very finite switches. So, in our case as we need the backup system the servo controller is best to initiate.

2.7.2 End Effector of the Robot

The end effector is one aspect that what brings the robot to give adaptable solutions[3]. This device is designed to have a great connection with the environment, and the working of end effector depends completely on the robot applications. Basically, the end effector is nothing but a gripper or a device that works according to different applications induced in it and when we consider it to robotic awareness. They are of different divisions like.

Impactive, Ingressive, Astrictive, Contigutive. These works differently for different end effectors.

Impactive: - This works as a jaw or fingernail that grasp physically by giving an explicit collision to the object that is to be acted.

Ingressive: - Use of pins, needles that helps in physically infiltrating the surface of the object. In my case I use vacuum cups to pick the sheet.

Astrictive: - It is nothing but the suction that is generated on the surface of the object, which is produced through vacuum cups as outsource and by electromagnetic stuff if in use.

Contigutive: - It is enforced to have a direct contact for the holding process of the object, for example surface tension generated at particular point.

So, these are the categories based on various physical belongings of the system. And in individual purpose depending on the working material like for metal sheets, vacuum cups or electromagnets play a dominant role as end effectors. In our case, we have taken into the consideration many factors and took an initiative to design suitable vacuum cups such that the sheet is picked firmly with a particular pressure exerted and is placed on the conveyor belt of the shearing operation without any uneven movement of the sheet.

2.8 Related Works

S. Pachaiyappan, M. Micheal Balraj and T. Sridhar have published a journal that contains complete data related to articulated arm robots for industrial applications[4]. They have developed an advanced technique in working of these particular robots from hazardous conditions and how the human can intervene into the robotic work zone. The ultimate motive in the research was to save human lives and in addition of increasing the productivity and quality of product with good and high technology environment. Nonetheless they have focused on safety and to create a good and healthy environment in the industry with use of advanced technology.

After a deep study, we have undergone many methods in development of articulated arm robots as pick and place operators related to our usage in the industry. The FANUC system has been taken into reference for developing a new robot according to the constrained environment and material of work [5]. The entire model is designed in Creo parametric 3.0, the Assembly and Simulation part is carried out in Autodesk Inventor 2017. As we have experience and knowledge about these tools earlier.

We have been introduced to robotic arm in JNTU Hyderabad (where we have earlier done our Bachelor's), and there we did a detail study on the manual of robot provided by FANUC. So, we have taken the dimensions based upon these manuals to develop our model, which are not exactly same dimensions according to FANUC standards, but have been modified slightly as we need to do relating to space constraints in SIG (Signode India Limited).

3 Design & Drafting

Design of robotic arm means the human supervision on this operation should be reduced. The shearing operation on which we are working can handle one sheet at a time. So, the first feature that is expected from this automation is picking up a single sheet from the stack of many sheets. There are many options to consider for this carrying operation. For example, a set of suction cups in a conveyor belt or suction cups replaced with electric magnets. We cannot use electric magnets as they might pick multiple sheets instead of one. The cutting blades cannot take more than one blade. Of course, it can cut those 2 at a time but the blades get worn out quickly. To make sure only one sheet gets picked up, we use suction cups. If at all we consider the possibility of making a robotic arm for the purpose of carrying the sheet, then our end effector should consist of suction cups. Between conveyor and robotic arm, we chose robotic arm for two reasons. First one was, robotic arm occupies less space when compared to a conveyor setup. In the industry, we are working, the place and position of this machine is so important. Just to install an extra enhancement, the whole shearing machine, which is very huge, cannot be replaced. So, to get fit into a small space, we thought that robotic arm would do better than a conveyor setup. The second reason was its portability. How easily it can be transported. Definitely, a robotic arm can be transported from one place to another quickly. So, considering all the above reasons, we decided to design a robotic arm with a pick and place type end effector.

The outline of the total mechanism was drawn on the paper just giving us the basic idea of the robotic arm which acts as a gateway to our imagination of how the shapes should be.

3.1 Mechanical Design

The most important aspect and backbone of this thesis is the mechanical design of the robotic arm. A robotic arm has certain design specifications and certain parameters are to be taken into the consideration. Since, the design is an area related to thought, many varieties of designs come to the mind at the initial stages of the design. Everything might not be fruitful

and the trial and error method cannot be trusted blindly. So, keeping all these things in mind, we have decided to design the robotic arm whose dimensions are loosely based on the dimension standards of Fanuc robotic arm. The basic points to be noted and followed for the design are[6]:

Functionality: The arm should have the ability to lift, move, lower and release an object while closely mimicking the motion of the human arm with full extension. Any device that can perform the required motions to pick and place an object required would have met the requirements of this criterion. The choice of the number of the parts in this particular robotic arm is taken by comparing it with a human arm. Let the action of human hand picking up a container appear in your mind. We have the waist, shoulder, elbow, arm, wrist and fingers do the job. This is the motivation for the choice of the number of parts. This robotic arm also has 5 parts and 5 joints which are pretty much like the human hand.

Reliability: The device should be able to consistently pick up and place objects in a smooth manner. i.e, the motion of the device should be smooth enough to not drop the objects that are being lifted. Therefore, any device that can lift and move an object from one place to another without losing any grip would meet the criteria. After a detailed study, the choice of end effector is made. Since, this device is used for picking and placing metal sheets, the first common thought any mind would get is that a magnet can be used to lift the sheet up. But the problem with that is, the thickness of the sheet is so small that there is a very high chance of more than one sheet being picked. If more than one sheet is fed to the shearing machine at a time, that hurts the shearing blade bad which can reduce the life of the blade. The next option in front of us was to use suction cups to lift the sheets. This is the most commonly used technique for the transportation metal sheets in industries all over the world. So, we had decided to use this technique for this purpose. Also, the industry also had the use of suction cups and a linear robot (conveyor) for the transportation of sheets in the printing process. So, we have enough motivation and data to use this technique.

Motion Range and Speed: Like human body the robots are constructed with same joints between bones, here we have a constrained limit for the movement of axis. In our design application, every particular axis has its own capacity of motion. The degree of movement of robot is calibrated from centre base of

axis. By this the speed in pick and place operation might vary, and this is occurred because each axis moves at different speeds. The complete motion of the operation is recorded in terms of degrees travelled per second.

Payload: The limited weight of each robot is its payload. So, the critical specifications and tooling weights are sotted out. In our application, this is useful in specifying different categories of robots by the above specifications.

Reach: In our articulated robot, we need to check the two extremities that is nothing but the V-reach and H-reach. Vertical reach is considered to know how high our robot can go in terms of height extension. Whereas the Horizontal reach is considered to know the distance of fully extended arm from base to wrist. In few other applications, we need to even consider a short Horizontal reach.

Axes: The distinctive segments of our robot are associated with mechanical joints, that serves as an axis of movement. We have designed our articulated robot with 5-axis of movement. Generally according to our knowledge industrial robots are designed to have 6-axis of movement, but the number and placement of robot just gives flexibility variation for each model.

3.2 Part 1

The first part designed in this project is this. It is because, based on its measurements we must measure remaining parts. And the weight of all other parts including the payload will have its great effect on this part since it is the base of this robotic arm. This part is an assembly of two different parts. Part 1 must rotate on its axis and other parts are connected to this. So, it is the main source of transportation. The two sub parts in this assembly are upper part and a shaft. The upper part is designed such that its bottom is the one side of an Oldham coupling as shown in the figure 3.2 below.

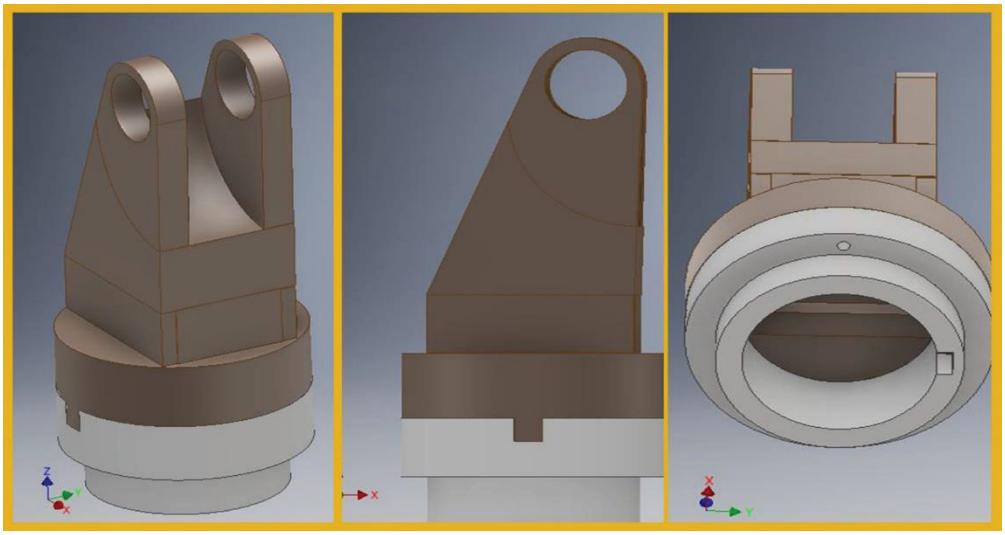

Figure 3.2.1: The upper part of Oldham Coupling.

The dimensions of this part are tabulated in the later part of the document. This part stays in the upper area of the base and will be visible. But there is a combination of shaft and key attached to this part from the bottom to which a power source is connected and is made to rotate. This supposed to be the component that transfers motion (rotational) from the power source to the upper part of the body. The shaft and key and the total assembly of the part 1 is shown in the figure below. The shaft and key inserted in this assembly acts as a typical Oldham coupling.

A general Oldham coupling has three flanges, one coupled to the input, one coupled to the output, and a middle disc that is joined to the first two by tongue and groove. The tongue and groove on one side is perpendicular to the tongue and groove on the other. The middle flange rotates around its centre at the same speed as the input and output shafts. Its centre traces a circular orbit, twice per rotation, around the midpoint between input and output shafts. For this operation, we modified the Oldham coupling a bit. Instead of using 3 flanges, we used only two, which are not flanges exactly. We designed the ends of the 2 parts in the base as Oldham couplings as shown in below figure 3.2.2.

Since this is a pick and place operation, two disc instead of three might be able to withstand the torque ranges of this operation. As we can see the lower part of Oldham coupling has a shaft and a key. The upper end of the

coupling has a flange which is directly designed with shoulder of the robotic arm. All the assembly described till now will be assigned a rotatory motion. That means, a motor is attached to the shaft at the lower most part in the figure below and if it rotates, the whole robotic arm rotates.

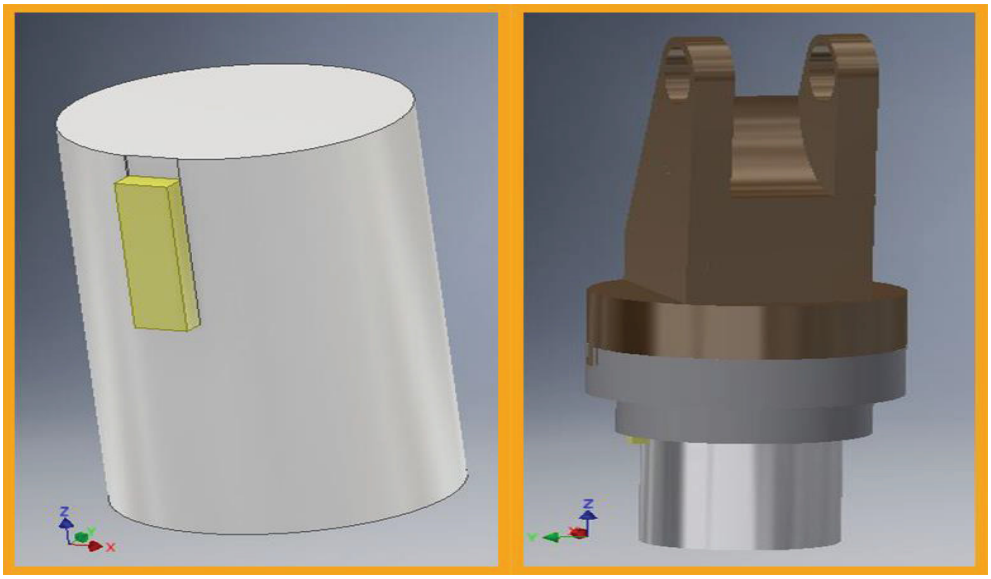

Figure 3.2.2: The shaft and Key of Oldham Coupling.

The dimensions of the shaft are given below.

Length of the shaft (L) = 0.182 meters

Radius of the shaft (r)= 0.12 meters

Volume of the shaft (V) = 0.002055 meters^3

3.3 Part 2

This part can be compared to the bicep of the human arm. Like the muscle of the human arm, it moves very less when compared to the forearm but it provides the strength and hold for the forearm and wrist to do their jobs. Its length is supposed to be more than part 1 and less than part 3 (since our design is like the human arm). An end of this arm is connected to part 1 creating joint 2 and the other end is connected to the part 3 to create joint 3. The design of this arm is shown below. The dimensions are tabulated in the later part of document. The upper end of the part is having a shaft to make itself rotate around the axis of the joint between part 1 and part 2. The lower end of this part is having holes and a gap between the two extended grooves to place the part 3 creating joint 3. The power source is connected to the shaft at the top end part 2. The rotation of this arm happens at this end. Its assembly, creating the joint and its limits are discussed in the assembly section. The dimensions of this part are given below.

Length of the part (L)= 0.45 meters

Thickness of the part (t) = 0.08 meters

Width of the part (b)= 0.153 meters

Volume of the part (V)= 0.00359787 meters^3

Area of the part (A)= 0.269904 meters^2

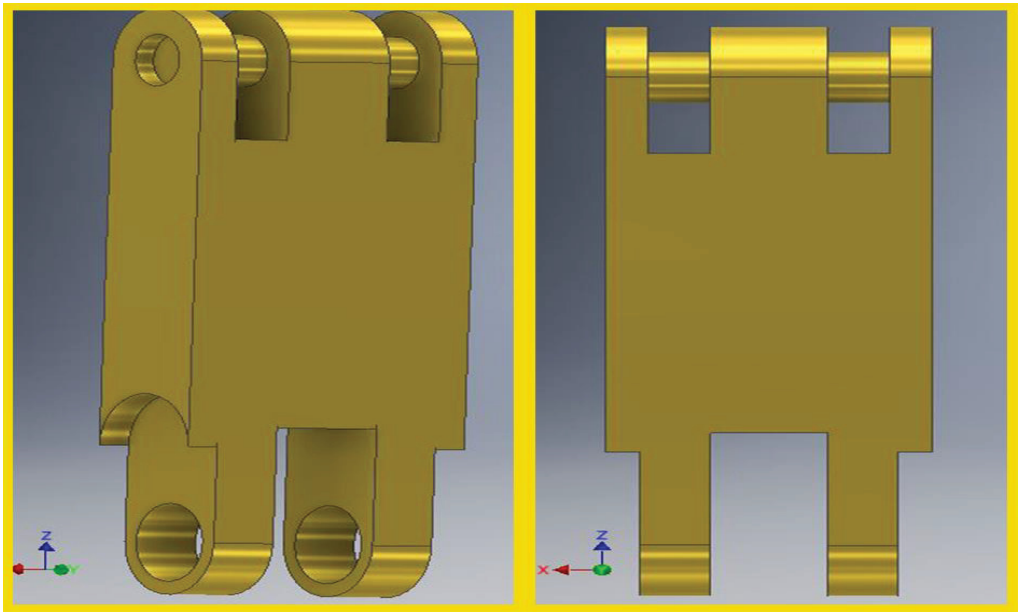

Figure 3.3.1: The CAD design of Part 2.

3.4 Part 3

This part is the forearm of this robotic arm. The reach of this robot mainly depends upon this part. This is a bit longer than part 2. The movement of this part is more when compared to the other parts. This part with part 2 creates a joint which is like the elbow in the human arm. The main purpose of these two arms is sustaining the weight that is lifted by the arm. One end of this arm is connected to part 2 as describe earlier. The other end is connected to part 4 which is a kind of wrist to this hand. The power source for this arm is given to the shaft on the left end in the picture below. The dimensions of this part are:

Length of the part (L)= 0.775 meters

Thickness of the part (t) = 0.08 meters

Width of the part (b)= 0.21 meters

Volume of the part (V)= 0.008741335 meters^3

Area of the part (A)= 0.488215 meters^2

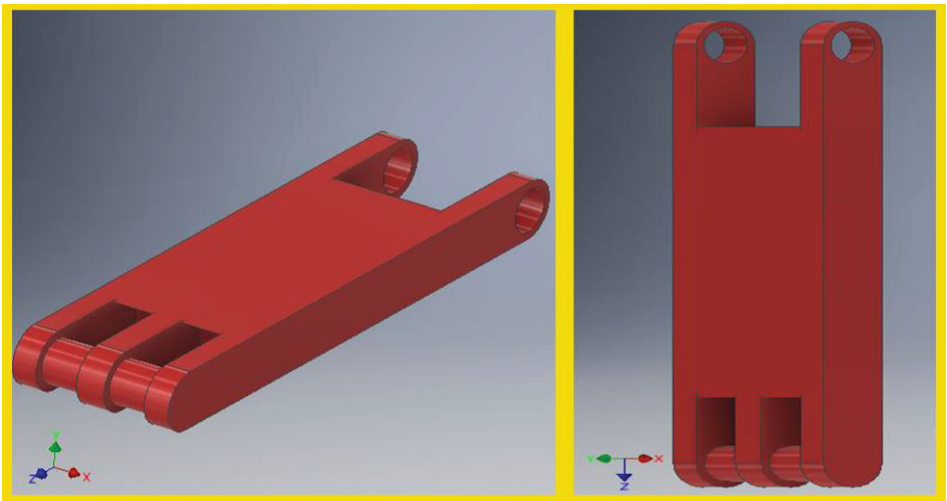

Figure 3.4.1: The CAD design of Part 3.

3.5 Part 4 & Part 5

Now we have arrived at the wrist part of the hand. Part 4 is the linkage itself between end effector and part 3. It has the ability to rotate around the axis at the end of part 3 (around X axis). It can rotate 360 degrees on the axis. How much it should rotate can be adjusted as per the requirement of the user. It also holds the end effecter (Part 5) in the desired position. It acts a joint for the part 5 where part 5 can rotate around its own axis (Y axis). The part 4 is shown in the figure 3.5 below on the left. Joint 4 is created between these 2 components. Part 4 being the stable one, it lets part 5 rotate around Y axis.

Length of Part 4 (L)= 0.266 meters

Height of Part 4 (H)= 0.155 meters

Volume of Part 4 (V)= 0.000875211 meters^3

Area of Part 4 (A)= 0.133435 meters^2

On the right of this picture, the part 5 can be seen. This is the one that rotates around Y axis. This part allows pneumatic cylinders to get connected to it. This part has the capacity to sustain the weight of 8 pneumatic cylinders and the sheet attached to them that is to be lifted. This part has the space to carry 8 more pneumatic cylinders. The dimensions of this part are:

Length of the part (L)= 0.75 meters

Height of the part (H)= 0.515 meters

Width of the part (b)= 0.5 meters

Volume of the part (V)= 0.005367438 meters^3

Area of the part (A)= 0.453101 meters^2

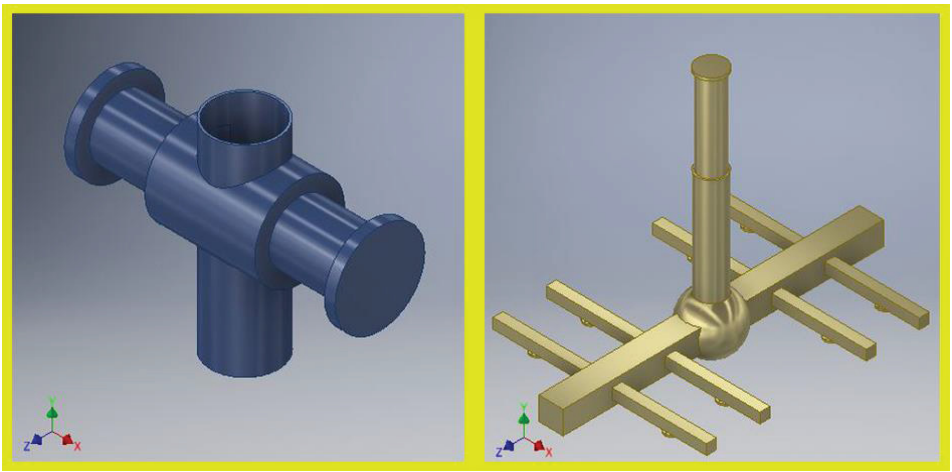

Figure 3.5.1: The CAD design of Part 4 and Part 5.

3.6 Pneumatic Cylinders

As we discussed earlier, the means of holding the sheet in this operation is executed with the help of suction cups and pneumatic cylinders. The phenomenon of this action is that; rubber suction cups get places on the sheet. And when ready, the air between the suction cup and the sheet is sucked out and a pressure near to the vacuum is created. The pressure outside the suction cup in way too larger than the pressure inside the cup. So, the air tries to enter inside the suction cup through the gap between the sheet and suction cup. This automatically creates an air lock and the sheet gets strongly attached to the suction cups. This phenomenon is already in use in the industry in the printing process which is already mentioned earlier. The pneumatic cylinder assembly is shown below.

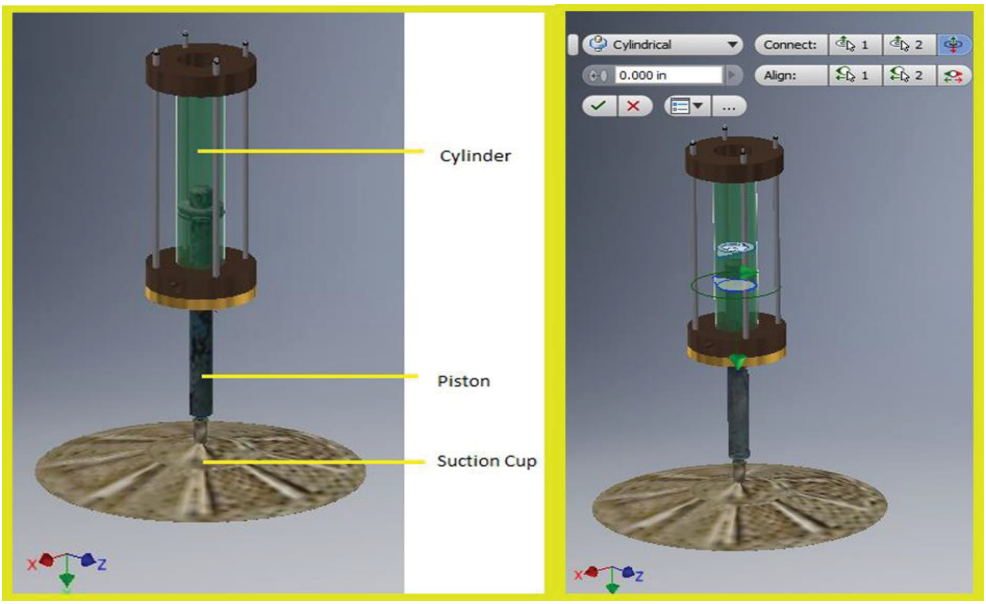

Figure 3.6.1: The CAD design of pneumatic Cylinder.

3.7 Assembly

After the design of individual part is developed in CREO Parametric 3.0 the next step is we need to assemble the parts to form a complete robotic arm using Autodesk Inventor 2017 Software[7]. The assembly has the arm with the wrist and end effector. If we describe the functionality of the robotic arm, it is a six degrees of freedom system. Six degrees of freedom (6DOF) refers to the freedom of movement of a rigid body in three-dimensional space. Specifically, the body is free to change position as forward/backward (surge), up/down (heave), left/right (sway) translation in three perpendicular axes, combined with changes in orientation through rotation about three perpendicular axes, often termed pitch, yaw, and roll. The part in the yellow rotates around its axis. The parts in red and brown are fixed at their bottom ends and move up and down. Now, the most important area of the robotic arm is described. It is the wrist and end effector.

And the dynamic behaviour of these assembled joints is explained below.

3.7.1 Joint 1 (Waist & Shoulder)

In the below figure 3.7.1, we can see 3 parts. The base is fixed which is obvious and the first part was coloured in black. Part 1, as marked in the figure 3.7.1, can rotate on its axis perpendicular to the base. How much it to rotate that must be decided by the user. The base does not rotate by itself. We use a power source which rotates the base. The base we designed might not be as simple as the outline shown below. The base area we designed consists of 3 parts. First one is the fixed, which provides a fixed support to the remaining moving arms. The second and third parts are the rotating ones. They are together assembled as shown on the figure 3.7.1. So, first the base part is to be fixed firmly to the ground and joint 1 is between the base and part1, the nature is it rotates around its common axis at a fixed limit of 0 to 360 degrees. The distance between part 1 and base is 1/8th of an inch and it is generated to avoid the friction between them, but we can set the gap between these two parts by an option in inventor. In the figure 3.7.1 below, the left one has a yellow arrow mark showing the direction of rotation and

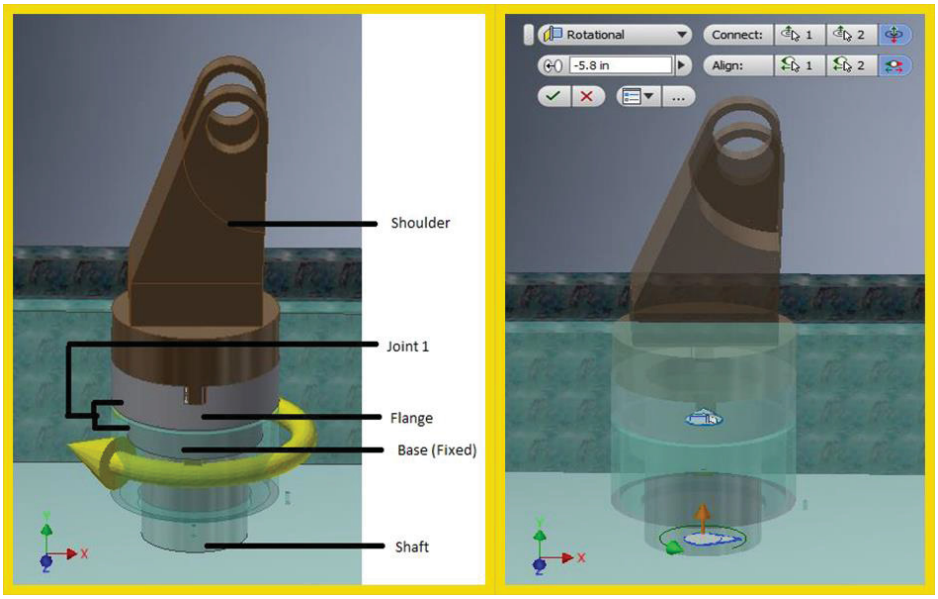

Figure 3.7.1: The CAD design of Joint 1 (Waist and Shoulder).

As we know the dimensions of the solid shaft the length, volume and radius, now to find the torque of the solid shaft we need to consider few other dimensions.

R= 0.958 meters

W= 33N

Where,

R is the distance of the radial arm from centre of shaft to maximum bending length of the arm.

W is the load acting on the shaft.

So, by considering the above dimensions the torque is to be calibrated.

Torque T= load acting on the shaft is multiplied to distance of the radial arm from centre of shaft to maximum bending length of the arm.

Therefore, the torque is T= W * R

T= 33 * 0.958

Torque of the solid shaft is = 31.614 Nm.

To know the stability of the shaft we need to find the FOS that is nothing but the Factor of Safety of a solid shaft.

We need to calculate Induced shear and allowable shear to find the Factor of Safety.

Induced Shear = $\frac{Torque*16}{\pi*d^3}$

Here, as we know the radius of the shaft is r = 0.12meters
Then the diameter is d = 0.24meters

Now, we need to substitute the calculated values in the formula above to find the induced shear of the shaft.

Therefore, Induced shear is = 31.614 * 16 / 3.14 *$(0.24)^3$

= 505.824 / 0.0434

= 11654.9 KPa

Induced shear is = 11.65 MPa

As we know the induced shear the allowable shear is to be taken form the ASME code depending upon the material we have considered.

So, according to ASME code for T6 6061 Aluminium material the allowable shear of solid shaft is calculated below.

The maximum shear stress should be 0.3 times tensile stress as per ASME code.

For T6 6061 aluminium alloy the tensile = 276 MPa
For T6 6061 aluminium alloy the UTS = 310 MPa
We must take the highest value that is UTS for calculating the allowable shear as per ASME code.

Allowable shear = 0.18 * 310

= 55.8 MPa

Therefore, the factor of safety is = allowable shear / Induced shear

= 55.8 / 11.65

The Factor of safety of a solid shaft is = 4.75

3.7.2 Joint 2

This is the joint that is formed by the combination of Part 1 and Part 2. Part 1 is associated to base with a joint (joint 1). This particular joint allows part 1 to rotate on its axis (Y axis). Now as part 2 is attached to part 1, part 2 can rotate on its axis (Z axis) in an up and down movement, and can rotate around the axis of part 1 (Y axis) simultaneously as both of these parts are connected. The anatomy of this joint is shown in the figure 3.7.2 below.

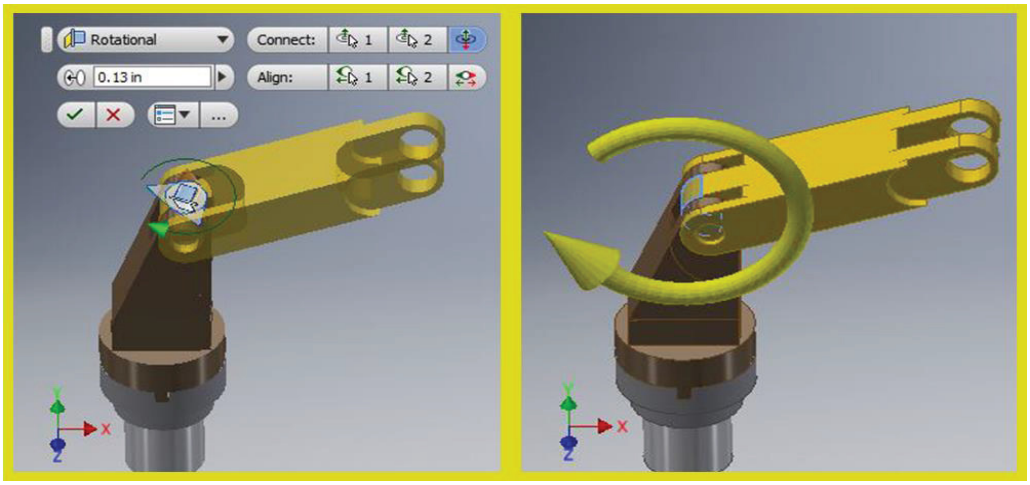

Figure 3.7.2: The CAD design of Joint 2.

The joint 2 has a fixed limit of rotation where part 2 (the part in yellow) rotates from 55 to 270 degrees. However, these limits are given such that both the parts consisting this joint do not collide. These can always be changed by the user. The gaps between walls of part 1 and part 2 are equal, and this is developed by avoiding all the possible contact among them, such that there is no proper friction development and the gap is also adjustable.

3.7.3 Joint 3 (Elbow)

The further anatomy of the robotic arm deals with the elbow. The elbow is the joint of two parts 2 and 3. The main purpose of this elbow is to give the arm some more room to move the end effector forward. Although each link in a robotic arm is important and must bare some weight, but this elbow is quite important as it can be termed as the centre of the robotic arm. The elbow is a joint of two parts which are shown below.

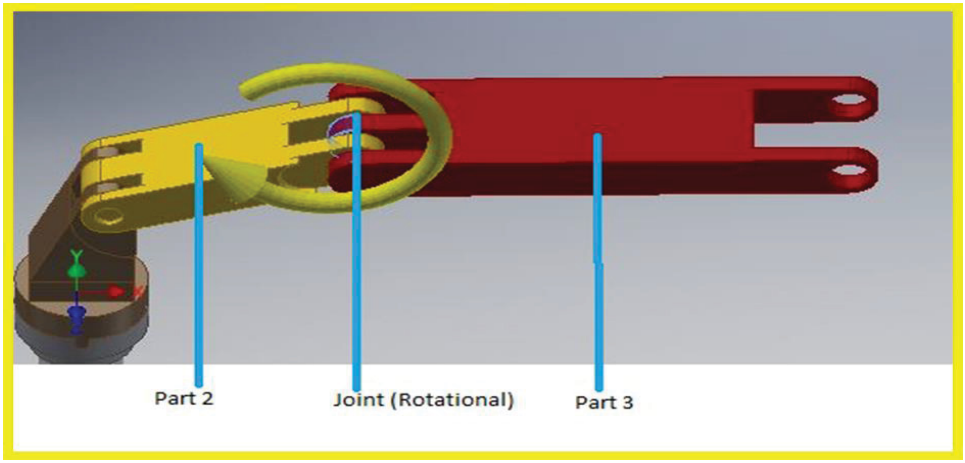

Figure 3.7.3: The CAD design of Joint 3 (Elbow).

These two parts are assembled to each other and their common point becomes the joint. Both of these are supposed to rotate around Z – axis i.e., they should move up and down. The yellow part shown in the figure is connected to the shoulder of the robotic arm shown above. This yellow part is continued with another arm in red as shown in the figure 3.7.3. Joint 3 has a fixed limit of rotation that is the red part moves on positive axis from 0 to 100 degrees and negative axis from 0 to –120 degrees.

3.7.4 Joint 4 (Wrist)

Wrist is the area which balances the operation. In this operation, the most important point is to balance the sheet while it is being transported. This robotic arm must pick a sheet and place it in another point. The picture below shows the top view of a prototype of the robotic arm. In this picture, there is a starting point and end point. The sheet is carried all the way from pick up point to end point. The most important point is, the sheet must remain parallel to the shearing surface all the time. The wrist plays an important role in doing this. The construction of this joint done in such a way that part 4 rotates around its axis (Z axis) and hold the end effector. Since part 4 is smaller in size when compared to part 3, it is important to balance the part 4 between

the groves of part 3. Improper balance might affect in non-uniform loading on part 3 and uneven deformation.

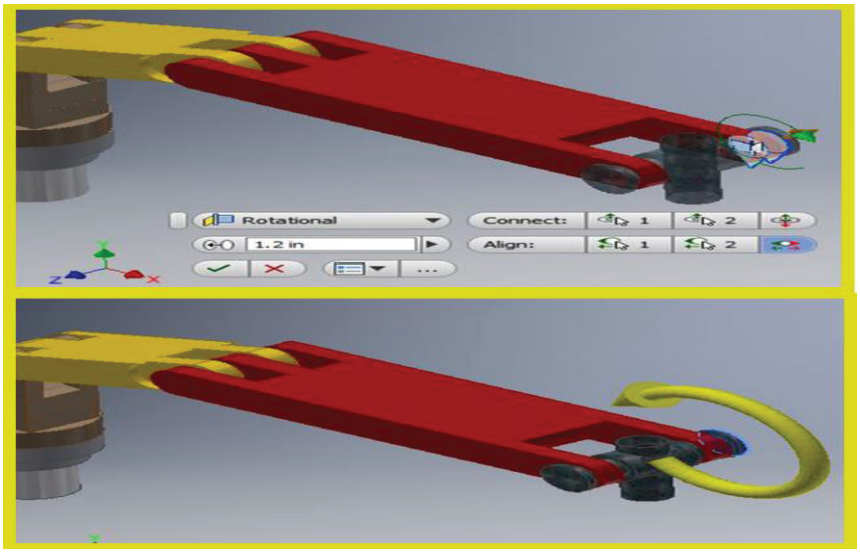

Figure 3.7.4: The CAD design Joint 4 (Wrist).

Joint 4 has a fixed limit of rotation that is positive axis from 0 to 230 degrees and negative axis from 0 to –20 degrees. In the part 2, 3 and part 4 are having joints in between them which are identical and its nature doesn't change.

3.7.5 Joint 5 (End Effector)

Joint 5 is the most important and delicate part of this whole assembly. This joint is between part 4 and part 5. Part 5 rotates around Y axis at the joint. Part 5 again needed to be assembled with the pneumatic cylinders. The movement of joint 5 is identical too joint 1 and hence the limits are also the same that is 0 to 360 degrees. In this the joint 1 and 5 are moving around y-axis and joints 2, 3 and 4 are moving around z-axis. In joints 6 we have eight pneumatic cylinders on the end effector as shown in figure 3.7.5, which means they consists of eight pistons and each piston is set into its respective cylinders with the same limits. The limits are (if the piston wall is in touch with topmost

wall of pneumatic cylinder and the movement is possible only downwards), the piston has a limit of 2.5 inch of maximum reach as 0.5 inch as the end, the same thing happens for the remaining seven pistons and thus the articulated arm is assembled. The figure 3.7.5 below is the full end effector which has 8 pneumatic cylinders and suction cups at its ends.

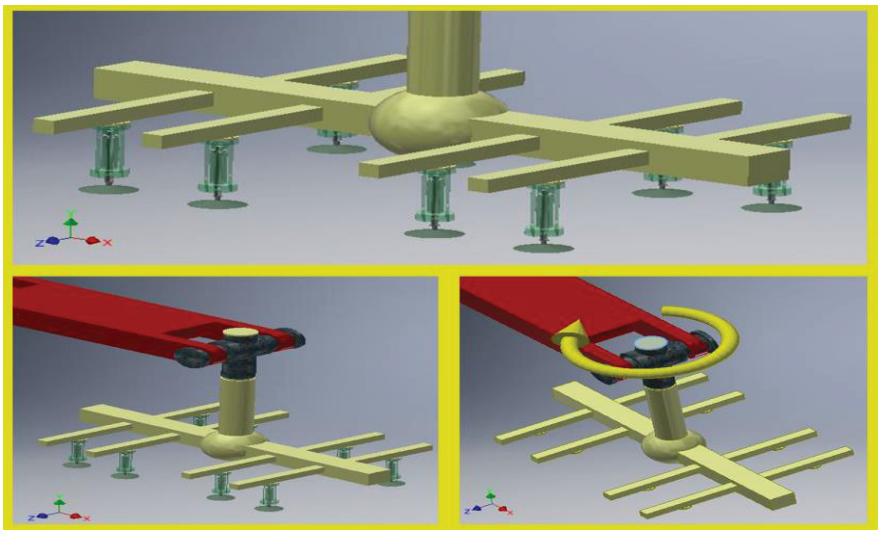

Figure 3.7.5: The CAD design of Joint 5 (End Effector).

All these joints assembled together gives the robotic arm, a pick and place operator. This robotic arm is now consisting of parts those are movable. Now, we must assign jobs for these parts. The main job is to pick and place a sheet metal from one position to another. This main job is divided into smaller jobs and assigned to each part and joint. Them working simultaneously as per directions given gets the job done. These set of directions explain dynamic behaviour of the robotic arm.

The complete Assembly of the Articulated Arm Robot is show in Figure 3.7.6. below.

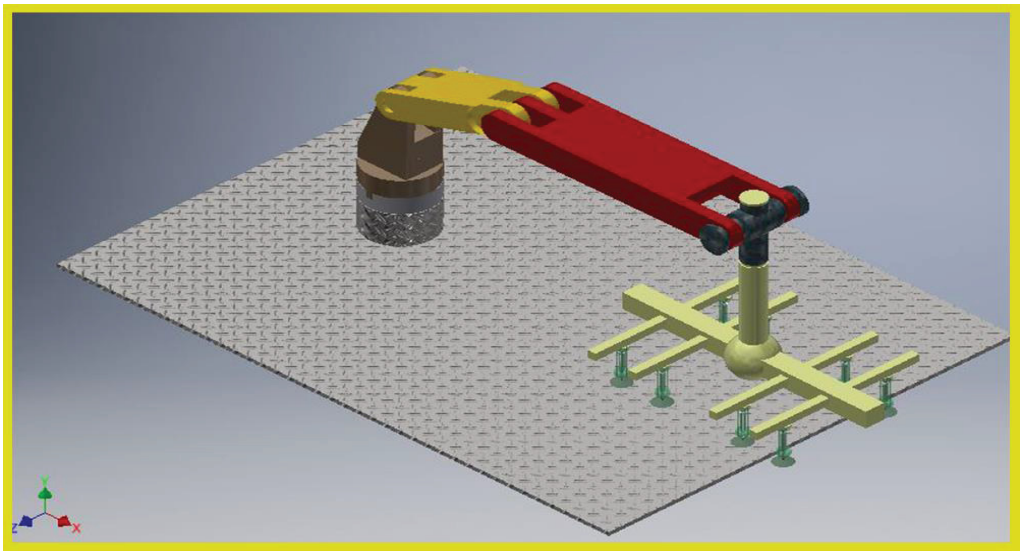

Figure 3.7.6:The Complete Assembly of Articulated Arm Robot.

3.8 Dynamic Behaviour of Robotic Arm

The very first job that is needed to be done is holding the sheet and getting ready to the take off. This work is done by the end effector. In our case, pistons of 8 pneumatic cylinders we have, shoot down and suction cups get themselves attached to the sheet. When they get attached to the sheet and an air lock is created between suction cups and the sheet, the piston rods retrace themselves into the cylinders creating a gap between ground or stack and the lifted sheet. This retracing action takes place in half a second, were this time is not a fixed. The user can edit the time as per his wish and requirements. These inputs are given in the dynamic simulation module[8] in Autodesk Inventor 2017. All proper assemblies created in Inventor are converted into required joints in the dynamic simulation module. For example, the piston is placed in the cylinder and constrain its motion limits such that it moves in between front and rear wall of the piston. This assembly is converted into a cylindrical joint in the dynamic simulation environment. Cylindrical joint has a nature where the part attached can move translationally and can rotate on its axis. This rotation is unwanted for our use here. Only translational motion is

desired. Autodesk Inventor provides an option to lock the DOF's using which we lock the rotational motion in this part. The total action of lifting the sheet up starts at 0 seconds and ends at 0.5 seconds. Now the next motion starts from 0.6^{th} second.

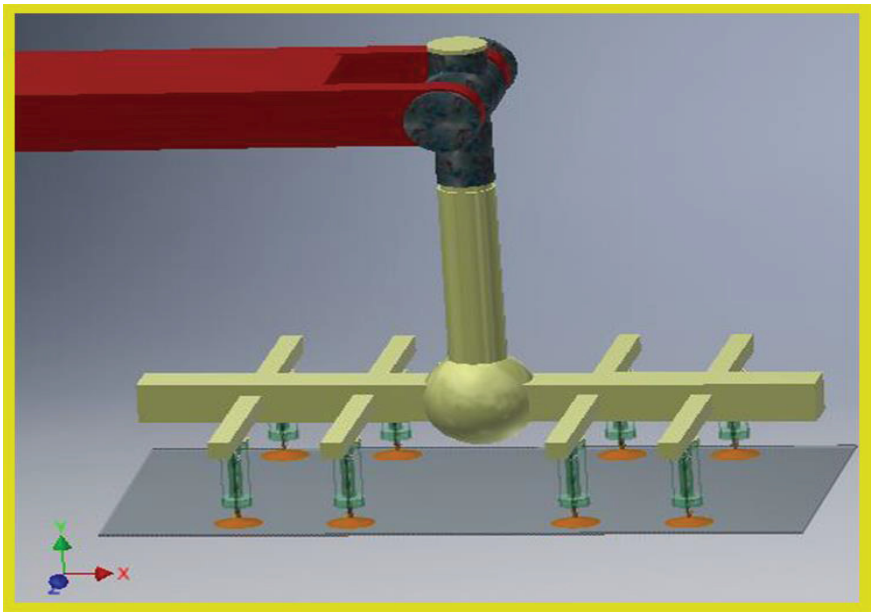

Figure 3.8.1:The dynamic behaviour of Pneumatic Cylinder.

The next job is to lift the sheet up to a safer height, so that it can be transported from one place to another. The word safe is used because, if it is not at a proper height the sheet might hit and collide with other machinery or may be any person standing near. This job of lifting it up is a result of simultaneous actions between part 2, part 3 and part 4. At 0.6^{th} second, part 2 starts moving upwards (Anti-clockwise direction). By the end of 2.5^{th} second, part two changes its position by 37 degrees. During this time period, there is a simultaneous movement in part 3. It also moves upwards changing its position by 10 degrees and then 20 degrees downwards. The reason of this up and down movement is that, there is a safe distance between end effector and the other parts of robotic arm. Collisions are messy but the movement of part 3 starts

from 0.7^{th} second. All these time limits and commands can be changed as per the user.

Now the most important task arrives, that is to try maximum how to maintain the sheet parallel to the ground (machining surface). The reason is, since the sheet is held based on an air lock between suction cups and the sheet. So, if the sheet is slant, it is forced to pull itself downwards and air lock can be broken. So, to avoid this and to maintain the hold, it is important to maintain the sheet parallel to the ground.

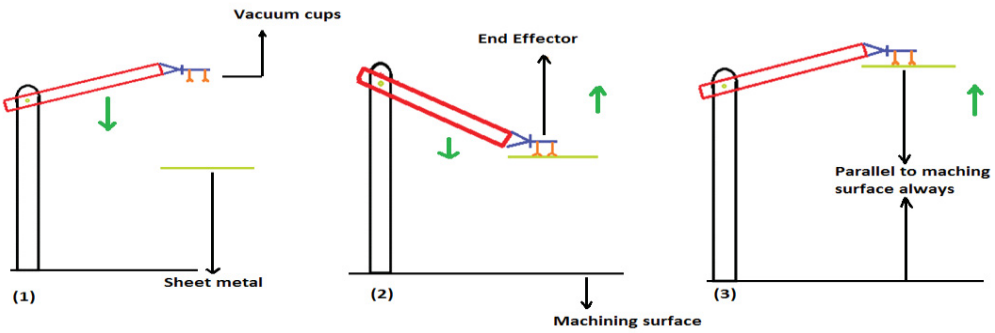

Figure 3.8.2: The Prototype of Robotic Arm in three sections.

Let us consider a human wrist while lifting and carrying a tray with glasses full of water in it. While lifting the tray, even though the arm moves upwards the position of the wrist changes with the motion to keep the tray parallel to the ground, so that the water won't spill. The same mechanism is being used here in the wrist. If we see the picture above, it is a rough sketch demonstration of the current action. We observe that the blue part and the sheet are parallel to the machining surface all the time. That blue part is part 4, which is described in the earlier sections. As part 2 and part 3 moves upwards or downwards, part 4 rotates in the opposite direction to put this sheet parallel to the ground. For this action from 0.6^{th} second to 2.5^{th} second, the part 4 to which end effector is connected rotates 28 degrees in clockwise direction. These three simultaneous actions lift the sheet up to the desired height and maintaining it parallel to the ground.

The next motion that follows is to transfer the sheet from its position to the destination. This is a solo action of joint 1, the rotational joint between base and part 1. The part 1 rotates and all other parts connected to it displace. This rotation starts at 2.5th second and ends at 5th second. The part 1 changes its position by rotating 90 degrees clockwise from its current position. But that is not the only task here. Let's observe the rough sketch below. It shows three steps of this action. In all these steps, the circle in the figure is the top view of the part 1. In section 1, the robotic arm is at its 2.5th second i.e. the starting point of rotation of part 1. Section 2 is its position during the travel and Section 3 shows the end point of this rotation (5th second). In all these three pictures, the sheet which is light green in the picture, always stayed in the same position with respect to the red line in the picture during the transportation. It only changes its position with respect to ground. This action is executed by the joint 5 (Rotational joint between part 4 and effector). As joint 1 starts acting, joint 5 also starts acting. The end effector rotates from 2.5th second to 5th second by 90 degrees, but in counter clockwise direction.

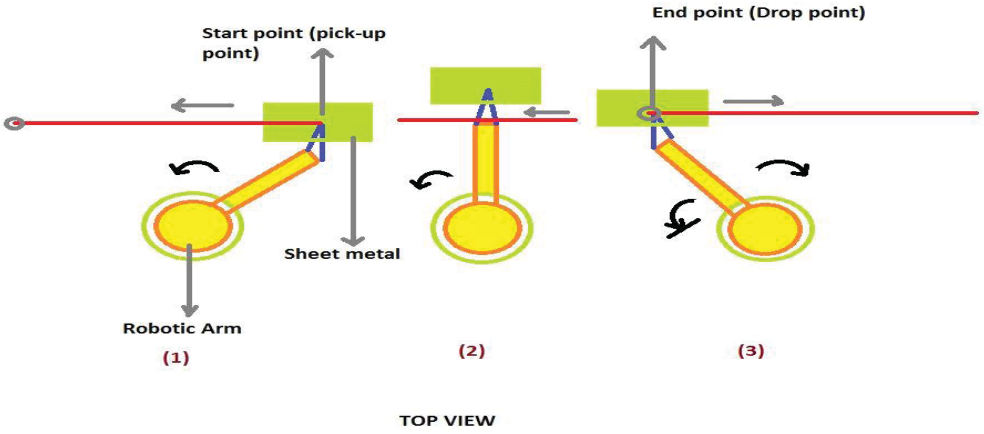

Figure 3.8.3: The Top view of Robotic Arm.

This particular action is assigned in this process only to test and verify the abilities of the robotic arm. These can always be changed by the user. As the sheet reaches the 5th second, the next task is to put it down. This action is again related to part 2, part 3 and part 4. This action is a mirror image of the

action of lifting up performed by these parts (0.6th second to 2.5th second) only difference will be the timing of this action. This action starts from 5th second and ends at 7th second. Again, the suction cups shoot down and put the sheet down. This action spans from 7th second to 7.5th second. As an example, the position vs time graph of part 2 is shown below. The whole action spans are for 7.5 seconds. The steps involved in assigning these positions and speeds at each joint is explained next.

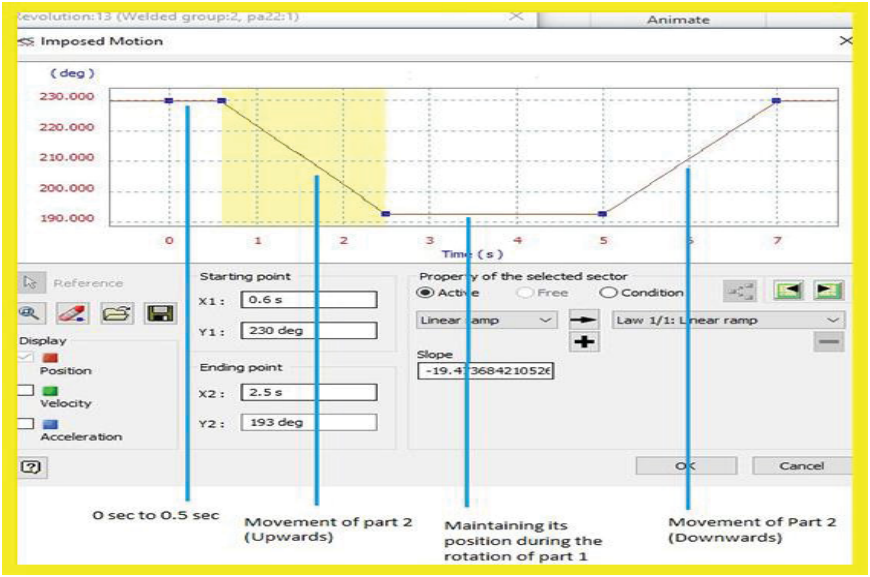

Figure 3.8.4: The Graph between Position vs Time.

In environments section in Autodesk Inventor 2017, there is the dynamic simulation module. Once it is opened, we can see a section called standard joints in model tree. This is obtained while performing the assembly. All joints that are assigned in the assembly are taken as standard joints. In our case, all the joints described above are present here. If these are unwanted or needed to be modified, there is an option available in this module. In bar the upper part of the screen, we find some option simulation settings. On clicking this, it gives an option Automatically convert constrains to standard joints. By clicking that off, we can edit our own joints in dynamic atmosphere using the

insert joint option in the upper part of the screen. Now it's just assigning the actions for every arm and coordinating their actions according to the job that is needed to be done. For example, select a joint in our case its joint 3 (Part 2 and part 3). Find this joint in standard joints section in model tree. Right click on it and select properties. Find edit DOF's option and start assigning the values either a numerical value or an input grapher. The process that is done for this joint is shown in a flow chart 3.8.5 below. Following these steps lead you to the command box shown in the following figure. We have the choices to edit the DOF's, change the path of a part or lock the DOF's such that the parts do not move at all. In this assembly for robotic arm, we have used rotational joints for joint 1, 2, 3 and 4 and we have used cylindrical joints between piston rods and pneumatic cylinders.

Now, let us see the construction of robotic arm in a flow chart below.

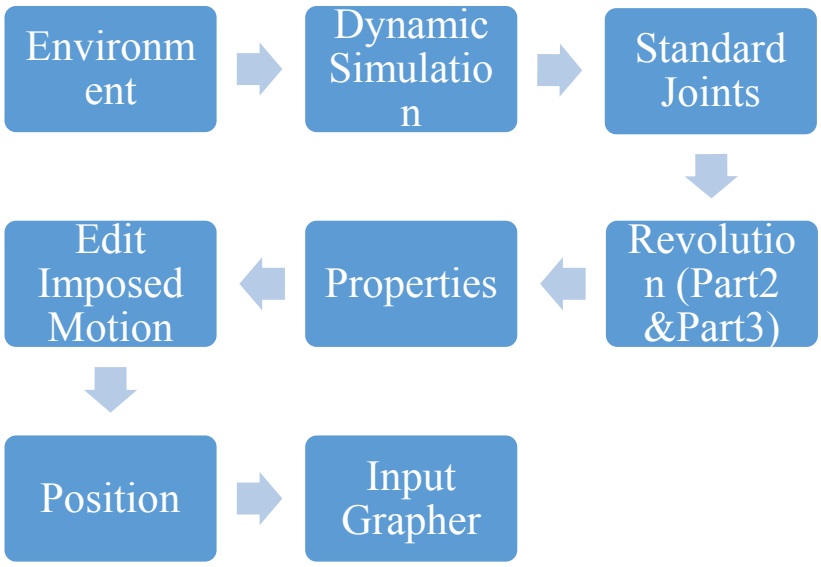

Figure 3.8.5: The flow chart construction of Robotic Arm.

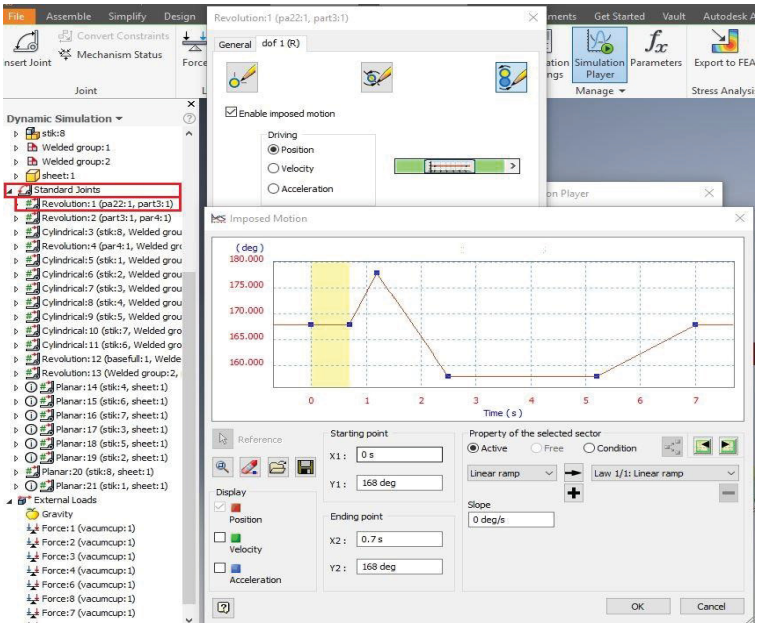

Figure 3.8.6: The Graph between Position vs speed.

4 Materials

Robots are mostly built of common materials. Some specialized robots for clean room applications, the space program, or other "high tech" projects they may use titanium metal and structural composites of carbon fibers. The operating environment and strength required are major factors in material selection[9]. There are a wide variety of metals and composites available in the market these days. Selection of material is very deep process. We have referred material and process charts designed by Mike Ashby[10]. He has provided us with a wide range of plots showing the different qualities and characteristics of materials plotted against each other. Of all them, we focused on 2 chats, strength vs density plot and strength vs relative cost figures 4.1 and 4.2. Selection of materials and the cost study to design an economic model is a completely different and deeper area of engineering. That case study requires more parameters to compare judge the choice of materials. We are not getting into that now but, we tried to choose the materials in such way that they satisfy our load bearing capacity requirements and not too expensive.

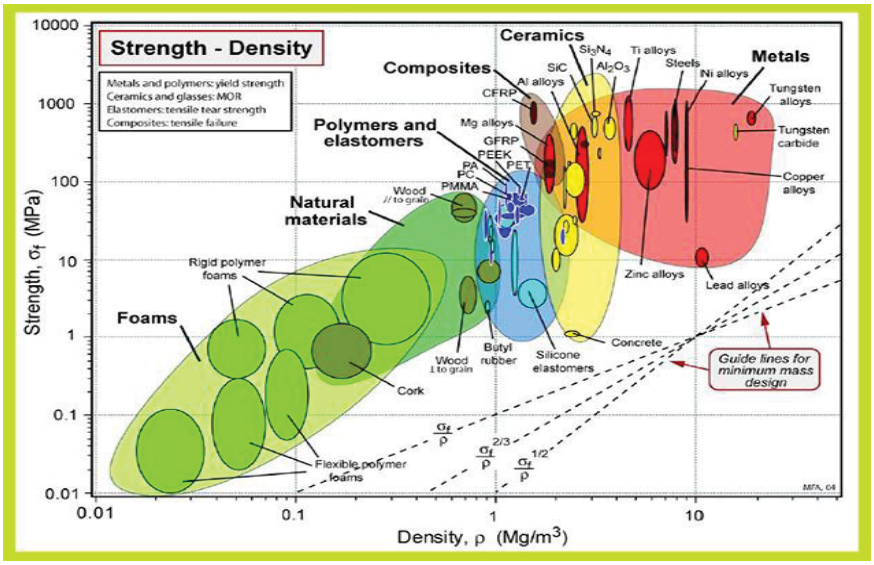

Figure 3.8.1: The Graph between Strength and Density of the Material **[10]**.

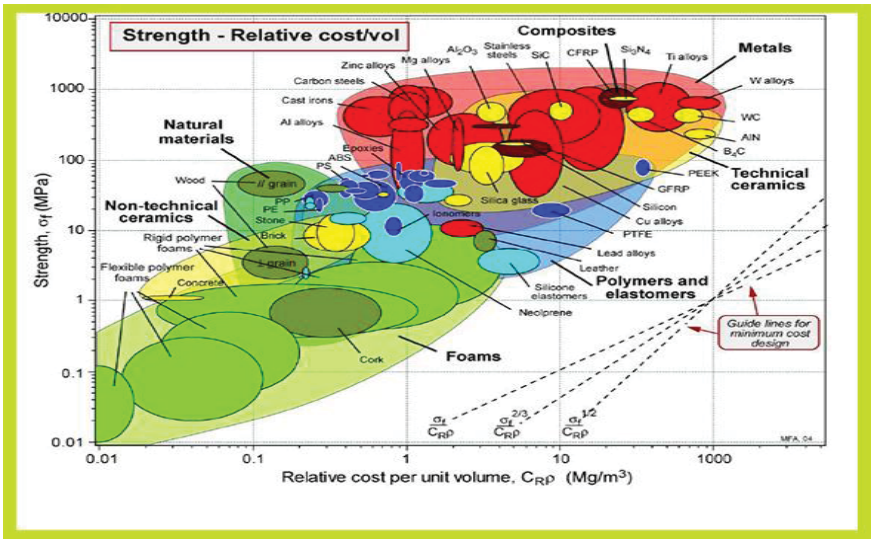

Figure 3.8.2: The Graph between Strength and Relative cost per unit volume[**10**].

Steel, cast iron and aluminium are most often used materials for the arms and bases of robots. Aluminium is a softer material and therefore easy to work with. But steel is several times stronger. We chose to design the parts with aluminium. It hasn't been a direct selection. The part 1 has a choice to have more weight when compared to other parts. The remaining parts are not grounded and needed to carry some weight of other arms and end effector also the sheet in this case. So, they cannot be heavier than the base which can harm the part 1. We decided to assign aluminium to all parts including part 1. Of course, we always have choice to change the material. Our selection has been proven good as aluminium did good for parts 1,2,3 and 4. But, in the opposite case, we decided to assign stainless steel to the parts. Only part 5 showed less load bearing capacity with aluminium but, we have tried changing the material to CFRP (Carbon Fiber Reinforced Polymer). The reason for this is it is stronger and lighter material than aluminium. We cannot assign a material with more density. As density increases, weight increases and increase in weight of Part 5 might have bad effects on other arms. Our experiment worked and the part 5 has increased its capacity in figure 4.3. The only problem with CFRP is it is relatively expensive. But again, selection of materials is a completely different study. We limit our study to the usage requirements of the industry.

The material used for most of the parts of robotic arm is Aluminium 6061 alloy[11]. Aluminium 6061 is a precipitation-hardened aluminium alloy, containing magnesium and silicon as its major alloying elements. It has good mechanical properties, exhibits good weldability, and is very commonly extruded (second in popularity only to 6063). It is one of the most common alloys of aluminium for general-purpose use. The mechanical properties of 6061 depend greatly on the temperature, or heat treatment, of the material. Young's Modulus is 69 GPa (10,000 ksi). Annealed 6061 (6061-O temper) has maximum tensile strength no more than 120 MPa (18,000 psi), and maximum yield strength not more than 55 MPa (8,000 psi). The material has elongation (stretch before ultimate failure) of 25–30%.

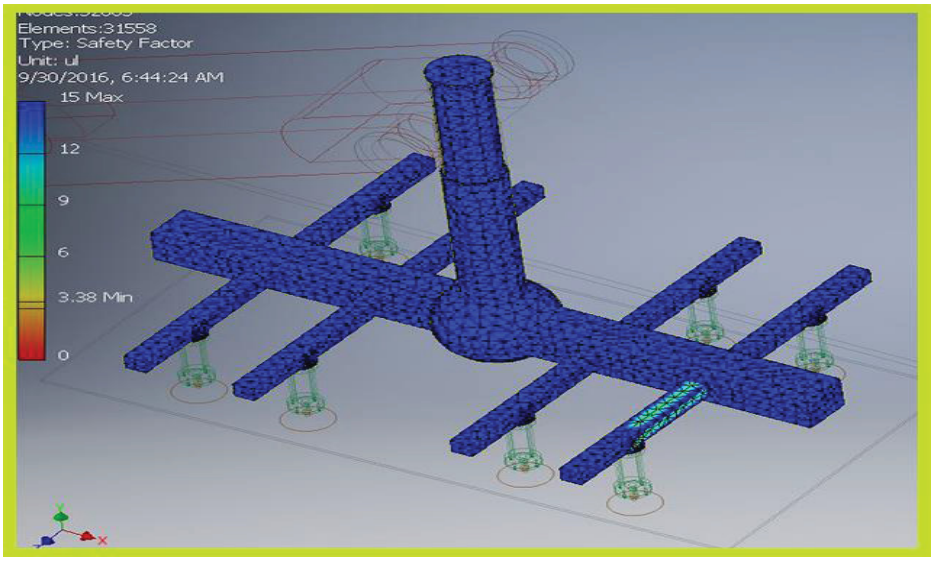

Figure 3.8.3:Part-5 assigned with CFRP material.

5 Simulation & Analysis

5.1 Need for Stress Analysis

A good design is always judged by its load bearing capacity. In operations like transport where machines are used, we expect them to be stronger than the necessity, so that they can perform the required action for a long time. Stress analysis is an engineering discipline that uses many methods to determine the stresses and strains in materials and structures subjected to forces. In engineering, stress analysis is often a tool rather than a goal; the ultimate goal being the design of structures and artifacts that can withstand a specified load, using the minimum amount of material or that satisfies some other optimality criterion. The stress on the part can be related with the load carrying capacity. Typically, the starting point for stress analysis is the geometrical description of the structure, the properties of the materials used for its parts, how the parts are joined, and the maximum or typical forces that are expected to be applied to the structure. The result of the study (analysis) is a description of how the applied forces spread throughout the structure, resulting in stresses, strains and the deflections of the entire structure and each component of that structure. The analysis may consider forces that vary with time, such as engine vibrations or the load of moving vehicles. In that case, the stresses and deformations will also be functions of time and space. Generally, the calculation of the stress distribution used to be carried out using mathematical means and Finite Element Methods. But calculation of stress distribution more appropriately needs more number of elements in the geometric design. This increases the computational time and effort by doing it only in the mathematical way. Hence, we take the aid of simulation techniques of CAD software's such as Autodesk Inventor 2017 to perform these tasks and save the effort. To establish a good simulation environment, we must apply proper loads and boundary conditions to make the model as close to reality as possible.

5.2 Loads & Boundary Conditions

The robotic arm has 5 joints and every joint has only one degree of freedom (rotational). To do this, we must specify an axis for each joint to rotate around it. Any other kinds of movement are constrained. The way the joints are created are explained in the Assembly section in the earlier part of the document. In this area, we discuss about the Behavior of the joints under loads and boundary conditions. The figure 3.7.2 shows joint 2 of the assembly. The joint has already been defined as the rotational joint. Now, for part 2 to rotate, a moment must act on the shaft of part 2. The angular momentum of an object can be connected to the angular velocity ω of the object (how fast it rotates about an axis) via the moment of inertia I (which depends on the shape and distribution of mass about the axis of rotation). The part 2 moves from 230 degrees to 193 degrees in anticlockwise direction for 37 degrees in two seconds giving the angular speed of 18.5 degrees/sec. The speeds of the joints are tabulated below table 5.2 for the calculation of moment.

Table 5.2.1: The table for Velocities of all Parts.

Part No.	Start point	End point	Time taken	Velocity
1	360 degrees	270 degrees	2.5 secs	36 deg/sec
2	230 degrees	193 degrees	2 secs	18.5 deg/sec
3	168 degrees	178 degrees	5 secs	20 deg/sec
4	186 degrees	214 degrees	1.2 secs	23.3 deg/sec
5	360 degrees	270 degrees	2.5 secs	36 deg/sec

The angular moment **L** can be calculated using the formula $\boldsymbol{L} = \boldsymbol{I} \times \boldsymbol{\omega}$, where $\boldsymbol{I}$ is the moment of Inertia of the body and $\boldsymbol{\omega}$ is the angular speed.

Inventor performs these calculations itself and takes the moment value for the calculation. Along with the speeds of the joints, we also give the loads on the end effector. The sheet is an Iron sheet with measurements 777×400×4 mm, mass of the sheet is 3.35 Kg and weight 32.9286 N. There are 8 suction cups on the end effector. The weight of the sheet acts downwards (due to gravity). The suction cups need to create a force that overcomes gravity. The only external loading given in this model is, the pressure acting on the sheet at the suction cups to lift the sheet up. As we said earlier, the suction cup phenomenon is already in practice in the industry. There the pressure created on the sheet in the direction against gravity by the locking of suction cups is 3 bar. In our case, we have 8 suction cups. This pressure is divided among 8 cups and is converted to force by multiplying the divided pressure with the area of the suction cup.

The overall pressure on the sheet is, P = 3 bar = 300000 Pa

Divided among 8 cups, pressure by each cup is, P_{cup} = 37,500 Pa

The area of the suction cup (Calculated from Creo) is, A_{sheet} = 0.00108 meter^2

Now, the force created at each cup is, F= Pressure x Area = 40.5078 N

The force F that is calculated above is the force that acts against gravity at one suction cup. There are 8 of them on the end effector so the net force against the gravity is 8 times F.

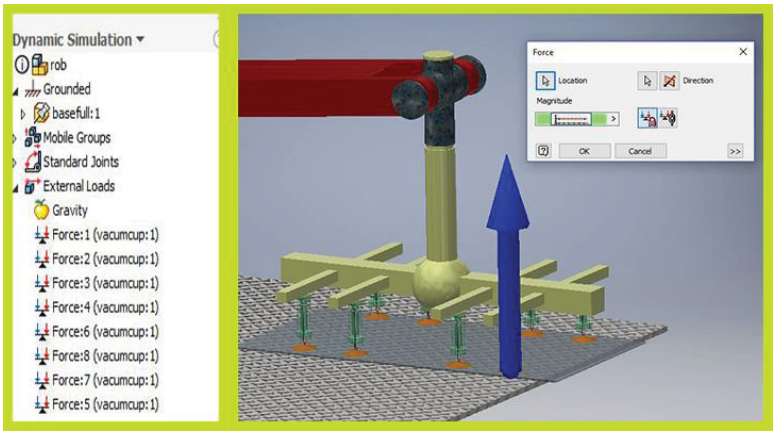

Figure 5.2.1: The Force acting on the sheet.

The remaining loading in this model is automatically taken from the assembly. The external loads are to be given separately.

5.3 Export to FEA Module

The dynamic simulation module only provides the means to learn and correct the dynamic behaviour of the assembly. We have provided the loads, forces and constraints needed for the robotic arm. There is a particular timing for each part and all of them moves correspondingly with each other. All the action happens in 7.5 seconds and the movement is solved for stress in stress analysis module.

As discussed earlier, all these components are to be exported to FEA to perform stress analysis. For this we have export to FEA option in Dynamic Simulation module. All that is needed to be done is selecting the part that is needed to be exported. Click on the export to FEA, then select a part or multiple parts. As soon as the parts get selected, a window opens asking to select all the joints and contacts related to it. For example, part 2 is selected to export. The links we have for part 2 are joint 2 and joint 3. We select the surfaces of part 2 that has direct contact with joint 2 and joint 3. Results can go really bad. The export to FEA module and selection for part 2 are shown in the figure below 0.1.

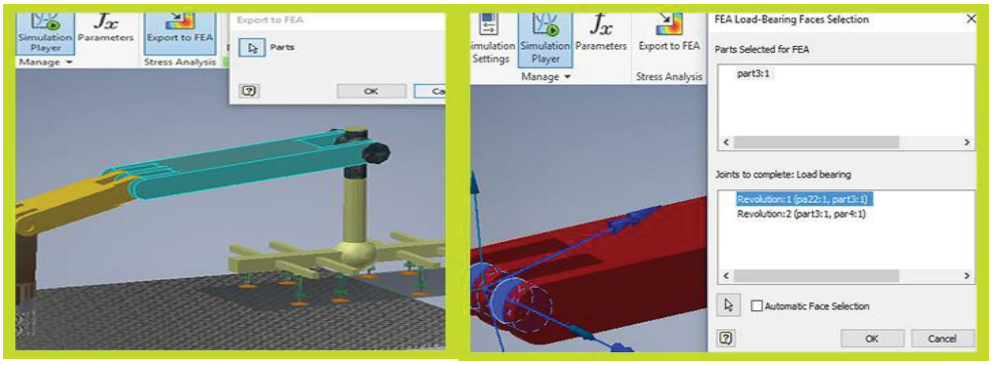

Figure 5.3.1: The Export to FEA.

Part 2 doesn't have any welded joints attached to it. Even though the selection is same for those components with the welded joints, here is the example of part 5 which is associated with joint 5 and has 8 pneumatic cylinder surfaces welded to it. The selection is shown in the figure below. It is important that the component that is to be exported must be a flexible one. That means, sometimes for our convenience, we assemble different components in different assembly atmospheres and join them under one atmosphere later. The final assembly which has sub-assemblies in it treats all the sub-assemblies as parts. So, to select a single part from a sub-assembly, we need to select that sub-assembly and right click on it, then select the option flexible on it. In this way, we select all the necessary parts that are exported to Stress analysis module in Autodesk Inventor.

After selection, run the simulation using the simulation player. In this case, the total time period is 7.5 seconds. After the simulation, has run, open the output grapher in the upper part of the screen. There we find the export to FEA option. Click that and we can see the parts that are selected for FEA. Now, we must generate a time series. Right click on the time series option and select generate series option. A window opens up showing the number of steps present between 0 and 7.5. We can select any number of time steps according to which we are going to analyse those parts. In the output grapher itself, we have all the stable groups, welded groups and standard joints present in it. Click any of the joint, select any option present there such as position, velocity and acceleration of that joint. Run the simulation and you can see the path of that particular physical quantity throughout the run time of the simulation. Which brings us to the point, the velocities or torques that are assigned for the joints with which they move.

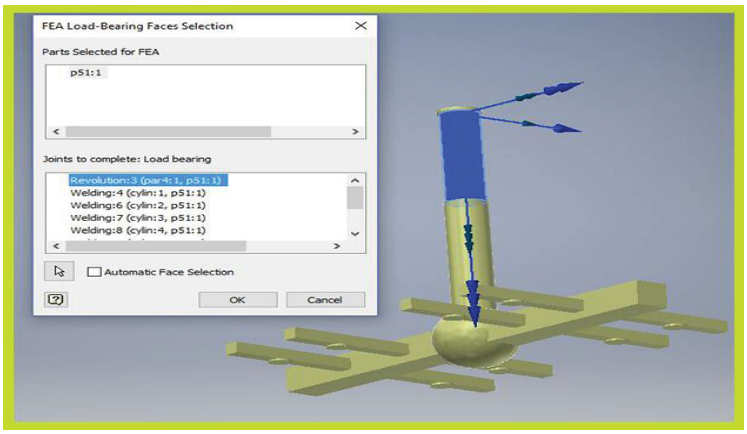

Figure 5.3.2: The Part-5 in Export to FEA.

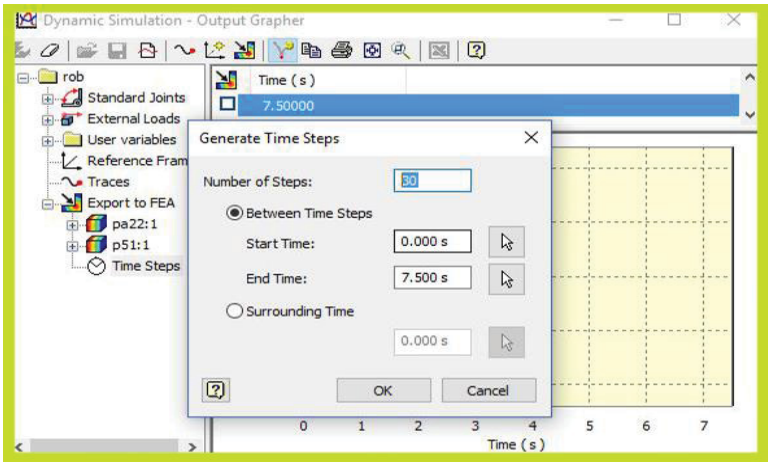

Figure 5.3.3: The Output Grapher and Time Series

Now, exit the dynamic simulation module and go to environment module. Go to stress analysis. Create the study, select the option motion loads. This option gives us the chance to select a particular part at a particular time. Here, for example, we chose part 2 to be simulated at the time 1.5^{th} second. Select that time or any time step closer to this value. Click ok and we enter the stress analysis environment. Here, the part which is going to be simulated appears as it is but all other parts in the assembly fades out. We can also see the yellow arrow marks all over the figure. Each arrow mark represents a load or force acting on that body. All the data is taken from the information

generated by the dynamic simulation. Now, we assign the materials for the parts here. Click materials section, go to assign materials and give each part a material which is desired. Here, we give aluminium for all parts except suction cups and sheet metal. Suction cups are given the rubber material and sheet metal is assigned with cast iron. The density of the material multiples itself with the volume of the part automatically giving the mass of the part. As the gravity is also assigned, the weight of the component is also added to the loads section. All this work is done by the software itself. The loads are given; constraints are set and materials are assigned. The next step is meshing. Go to the mesh controls, edit mesh size and click mesh view. The mesh is generated. Now, check for geometry updates such as contacts. Update contacts if necessary and run the simulation. Now, we arrive at the most interesting part, interpretation of results.

5.4 Meshing

The meshing of the designed articulated arm robot is accomplished very cautiously to achieve good amount of stress distributions. The stresses generated here are very high and these stresses are developed due to bending loads at the round and sharp corners. And by having a deep study about articulated arm robot cautiously, the high stresses generated are calibrated and are characterized as detracting ranges.

By default, meshing provided by inventor is made and the part is simulated, after the detail study of this stress distribution obtained. We found some areas were stresses are more when compared to remaining areas. The initial sizes of mesh are 0.1 minimum element size and the average element size is 0.2. Then the local mesh area option present in inventor to select the areas those are observed to possess high stresses and their element dimensions are changed to 0.01 minimum element size and 0.02 average element size. The local mesh control gives us the option to edit the density if mesh at any chosen area. The mesh adjusts itself according to the shape of the geometry. The shape of the element is tetrahedral and during the final stages of simulation, we made sure that each geometry has at least 2 lakh elements. The meshed Finite element model is shown in Figures below 5.4 and 5.4.1.

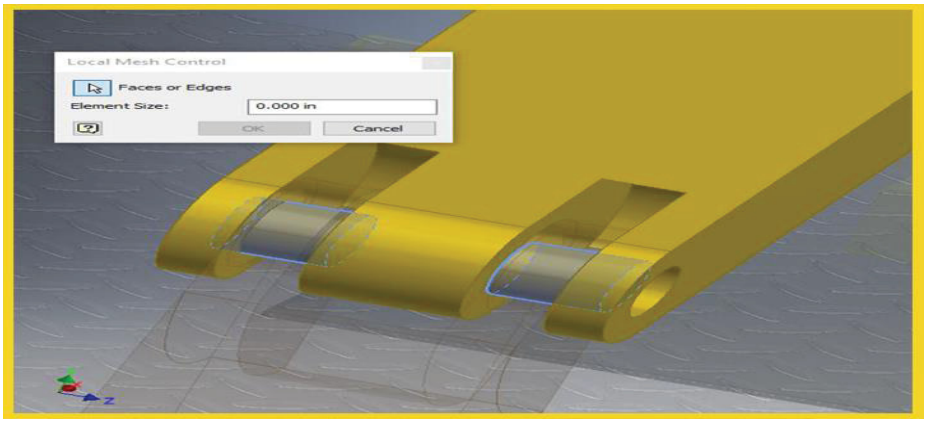

Figure 5.4.1: The Joint were the meshing is excited

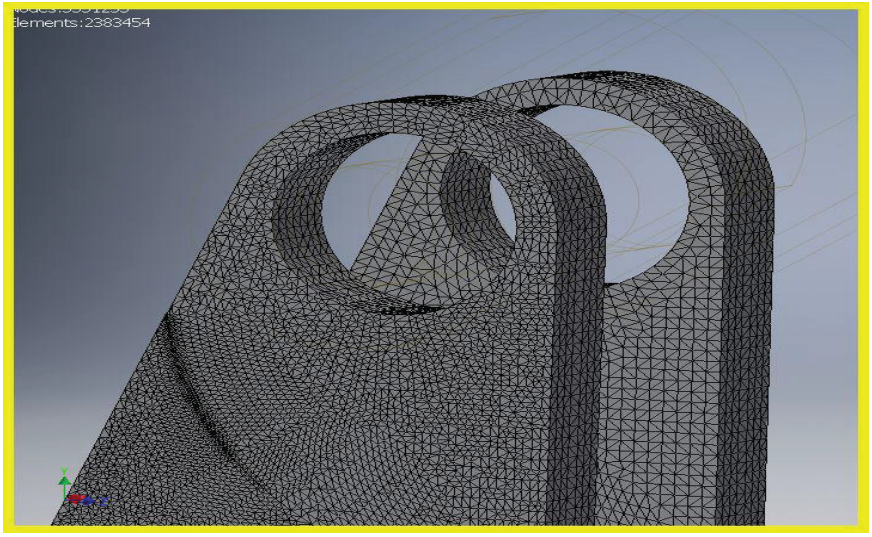

Figure 5.4.2: The Meshed Part of FEA.

5.5 Stress Analysis Environment

The Finite element analysis in Autodesk Inventor becomes really easy when the assembly is proper and the joint forces, loads and constraints are

given properly. The joints and parts are described and the way they are assembled is explained in the previous section. In this section, we discuss about the finite element analysis performed by the Autodesk Inventor on our robot. For this, we have exported the parts from dynamic simulation module to stress analysis module[12]. The movement of each and every part of robotic arm is preloaded and exported to FEA. The constraint set is very important for any structural analysis of any physical structure. If we have a load acting on a body, there must be a reaction of that load on that body. Physical constraints determine that reaction. For example, let us consider a cantilever beam with a load acting on its free end. Naturally, the deformation will be more at the free end. But its reaction is learnt at the constrained end. So, the strength and stiffness of that beam for that material is learnt.

Similarly, we constrain the components of the robotic arm according to our use. Each arm in the robot is involved in at least one joint. Even though the connections won't change during the process, the orientation of stresses on the components change due to their motion in the given time. Inventor provides the option of motion loads in stress analysis module. Where we analyse each part at any interval of time including the external loads, body loads and gravity. We just must generate a time series with the number of time steps between them. In this case, we have taken 25 time steps between 0 and 7.5 seconds. We choose 6 time points where we feel the change in the stresses and displacements can be observed clearly. The loading in this model is automatically taken from the assembly. The stress is analysed dynamically as we must know how the stresses are fluctuating in a part during its motion. The loads and boundary conditions change and recorrect themselves whenever there is the change in the position or time step. Now, we will have a stress distribution once the simulation is done. But, how do we know whether the results obtained are correct or at least approximately correct? Even if they are correct, are the results good enough to say that the design can take the load. Let's have this discussion in the coming sections.

6 Analytical Model

The hand calculations are performed in this case are just to verify whether the simulation is going according to solid mechanics theory. Since it is very tough and complicated to establish a 3D model with hand calculations, we always prefer simulation software's of FEA (Like Autodesk Inventor 2017). But to verify whether the given boundary conditions and created environment is correct, we tried to establish a deformation equation for a part in our model. Here we are going to compare the calculated value to the displacement (deformation) in x-direction in the simulation.

For this purpose, we take part-2 to carry on the hand calculations with in. we have few changes in the geometry of this part, such as we have ignored gaps and holes in the geometry and haven taken it has a solid linear beam with uniform cross section. The curved cross section is taken has a straight line. The dimensions of part-2 are given below.

Volume V = 0.00359787 meters^3

Density ρ = 2700 kg/meters^3

Mass M = volume * density

= 9.714 kg

Weight q = mass * g = 95.29N

Length L = 0.45 meters

b = 0.153 and h = 0.08

Euler-Bernoulli Beam theory

Euler-Bernoulli beam theory is a simplification of the linear theory of elasticity which can calculate load carrying and deflection characteristics of beam. We start with a 4th order differential equation of deflection and derive the 1st order equation. For this purpose, we take the position of beam at 0.5th second and assume it as a simply supported beam, with both ends fixed[13].

The boundary conditions of a simply supported beam are.

- *w (0) =0.* Because the beam is pinned to its support, the beam cannot experience deflection at the left-hand support.
- *w(L)=0.* The beam is also pinned at the right-hand support.
- *w''(0) =0.* As for the cantilevered beam, this boundary condition says that the beam is free to rotate and does not experience any torque. In real life, there is usually a small torque due to friction between the beam and its pin, but if the pin is well-greased, this torque may be ignored.
- *w''(L)=0.* In the same way, the beam does not experience and bending moments on its right-hand attachment.

The Euler-Bernoulli beam equation is given as

$$EI\frac{d^4w}{dx^4} = \frac{q}{L}(x)$$

On integrating the Euler-Bernoulli beam equation we get the derived equations as follows.

$$\boldsymbol{EI\frac{d^3w}{dx^3} = \frac{q}{L} * \frac{x^2}{2} + c_1} \quad (1)$$

$$\boldsymbol{EI\frac{d^2w}{dx^2} = \frac{q}{L} * \frac{x^3}{6} + c_1x + c_2} \quad (2)$$

$$\boldsymbol{EI\frac{dw}{dx} = \frac{q}{L} * \frac{x^4}{24} + c_1\frac{x^2}{2} + c_2x + c_3} \quad (3)$$

$$\boldsymbol{EI * w(x) = \frac{q}{L} * \frac{x^5}{120} + c_1\frac{x^3}{6} + c_2\frac{x^2}{2} + c_3x + c_4} \quad (4)$$

Now, let us consider that the load acting on the beam is uniformly distributed. So, to calculate the load at a particular point on the beam the function we use is

$$\frac{q}{L}(x)$$

Where,

(x = 0.1 to L)

Applying the boundary conditions in the above equation (4), we get the values of constants by using the MATLAB software as.

C_1 = -71.4726, C_2 = 0, C_3= 1.6885, C_4 = 0

After solving this in MATLAB we came up with a graph showing maximum deformation at the center.

The value obtained is $5.3*10^{-7}$m, but the obtained value at the center of beam in simulation of part-2 is $6.83*10^{-7}$m which is close. But if we observe more closely the deflection obtained from hand calculation is lesser than the one which we obtained from simulation.

They are many reasons for that, it might be loading because our loading is very approximate taken for the convenience of calculation. While the simulation environment might have more realistic loading. The other reason might be the material (density). For our mathematical model we have ignored all the groves and holes and took the beam as normal solid beam, but where it has multiple grooves and holes more material (density) means less deflection. With all these observations and results, we can say the simulation performed is close to reality and are logical.

7 Results & Discussions

7.1 Stress Analysis Results

The ultimate purpose of any analysis is to allow the comparison of the developed stresses, strains, and deflections with those that are allowed by the design criteria. All structures, and components therefore, must obviously be designed to have a capacity greater than what is expected to develop during the structure's use to obviate failure. The stress that is calculated to develop in a member is compared to the strength of the material from which the member is made by calculating the ratio of the strength of the material to the calculated stress. But, before the simulation, one must be able to figure out where the maximum deflection occurs in a part provided you have the information of boundary conditions. For example, if I see a cantilever beam with a load acting on it downwards, I can figure out that the maximum deflection would be at the free end and there would be a reaction force present at the fixed end acting opposite to the load. Similarly, we know the boundary conditions and loads acting on each part at every time step. Therefore, we have some idea where maximum deflection is going to be.

The Autodesk Inventor gives the stress distribution or deformation over the part at a particular instant. If I want the stress distribution at a particular time step, say 4.3rd second, I can edit the study properties, change the time step and re-simulate it. But, Inventor doesn't give the behavior of stresses along with time. That means, we cannot able to see a Time vs Stress plot in Inventor. So, just to understand the behavior of the stresses in a cycle and to find out where the stresses are maximum or minimum in the cycle, we have found out a way. The output grapher in the Dynamic simulation module of Autodesk Inventor, we can find the model tree of all the part, joints, stable parts, forces arranged there. By clicking any of them gives the option to view its plot against time. Here, we arrive at joints and select a joint. If we open that joint, we can find sub columns of position, velocity, acceleration, imposed force and moment, each having their plot against time throughout the cycle. We select the moment graph. The reason behind selecting the moment graph is,

We know that,

$$\frac{M}{I} = \frac{E}{\rho}$$

Where M is the moment,

E is the Young's modulus of the material,

I is the Moment of Inertia and

ρ is the density of the material

The stress denoted by $\sigma(y)$, can be written as the following equation,

$$\sigma(y) = \frac{-E(y)}{\rho}$$

The term $\frac{E}{\rho}$ replaced by $\frac{M}{I}$ gives

$$\sigma(y) = \frac{-M(y)}{I}$$

In the above equation, the moment of inertia is a constant value as the dimensions of the part remain same over the cycle. Therefore, the moment is proportional to the stress. Moreover, if we consider any part in the robotic arm, the maximum deflection is always at the closer to the joints i.e.; at the ends. The moment of the rotating part creates the deflections at those particular areas. Considering all these reasons, we can say that the Time vs Stress plot will be like Time vs Moment plot. But, to validate our assumption, we have provided with the following information. The Time vs Stress graph of Part 1 is shown below figure 7.1. We have simulated the part 1 in all the 30 time steps and plot the obtained maximum stress values against time steps. Both are shown below figure 7.1. They are not exactly similar because the Time vs Stress plot is generated by plotting 30 time steps against the respective stress values in Matlab. But the graph generated by Inventor is finer and definitely has more than 30 time steps. So, we can see more smooth curve than the one generated by the Matlab. But, the time steps where maximum and minimum values of

stress occur and time steps where maximum and minimum moment acts are the same.

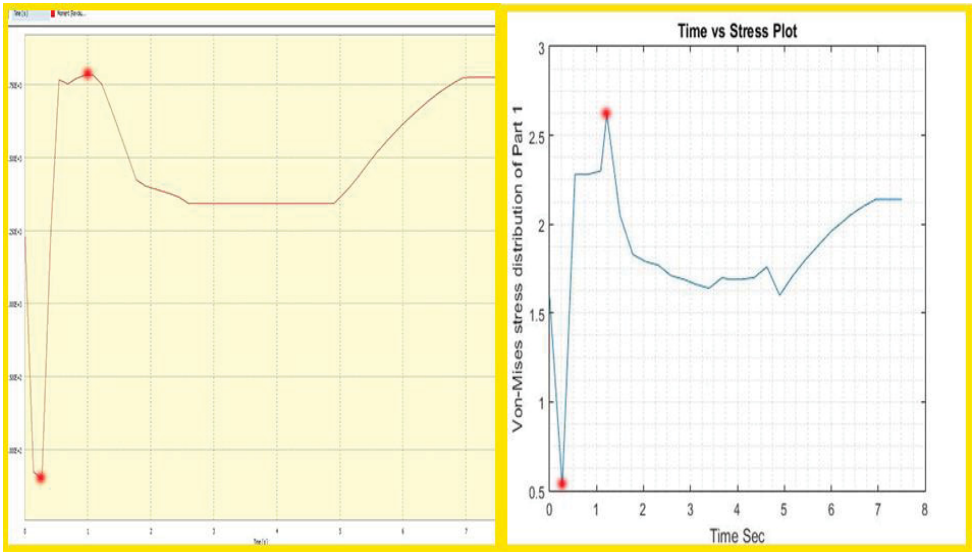

Figure 7.1.1: The graph between Time (sec) vs Stress of Part 1.

This supports our assumption. As simulating each part for 30 times and recording the stress values is a complicated process, we can use Time vs Moment plots to check those particular time steps where stresses are maximum and minimum. To check this again, we have done all the process explained above for part 2 also. Those two plots are also shown to be similar, making our point stronger. The comparison is shown in appendix. But, a different process for Part 5 is applied. There are 8 suction cups on Part 5 and the forces acting on those 8 cups is same. But change in the position of the sheet with time changes the behavior of forces are moments on Part 5. But all those Force vs Time graphs and Moment vs Time graphs for Part 5 have their peak and lowest values at the same point for all the suction cups. We can find the maximum and minimum time steps using those figures which are shown below figure 7.1.1.

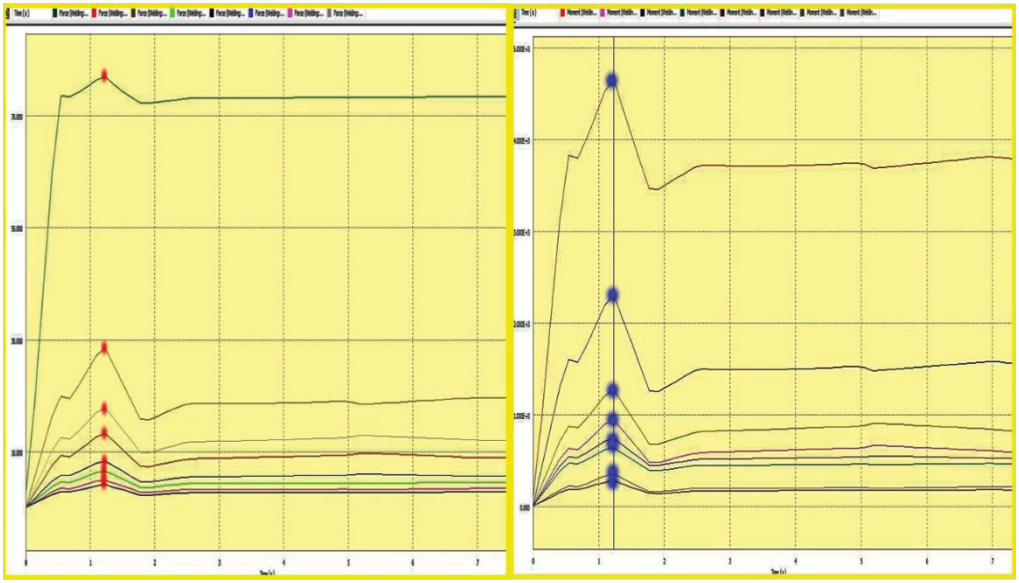

Figure 7.1.2: The graphs between Time (sec) vs force and moment.

The figure 7.1.2 below shows the stress distribution of Part 1. The stress as expected, is maximum at the top where it forms a joint with part 2. Part 2 has a shaft that rotates inside the holes provided in the top of part 1. The movement of part 2 induce stresses on part 1 on the top. There are also stresses in the remaining part of the body. Complete blue color doesn't say that there are no stresses present at all. The division of these stress ranges over the scale can be edited using the color plot option in inventor. Reduce the maximum value and more detail stress distribution is seen. The maximum stress on this part is 2.101 KSI which is equal to 14.48 MPa.

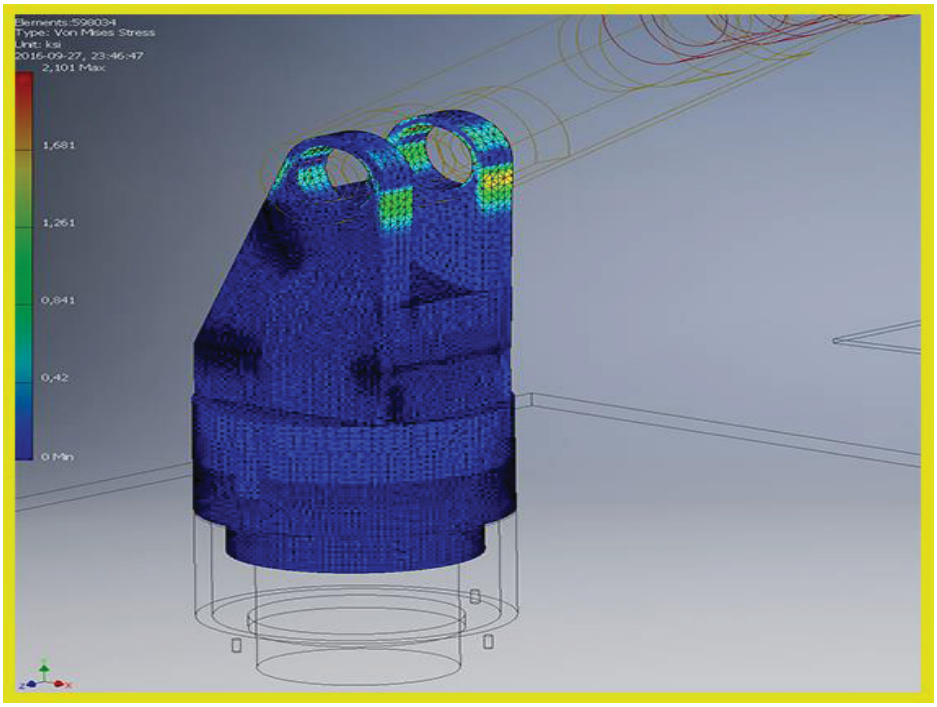

Figure 7.1.3: The stress distribution plot of Part 1.

Similarly, as shown in the figure (load section) in the Loads section, Part 2 is also connected with a part on both of its ends. The right end of Part 2 is connected with Part 3. Therefore, the moment on the Part 3 shaft which makes it rotate, have its effect on deflection in Part 2. Also, Part 2 is connected to Part 1. So, the maximum stress values are developed at both the ends of Part 2. In the same way, Part 3 is also connected with a part at each end. The kind of forces that are acting on Part 3 are like part 2. The most important observation form the stress distribution pictures down here is that the critical areas (where stresses are maximum) are found out to be at the ends of both Part 2 and Part 3, not anywhere in the middle. As we have discussed earlier, we expect the critical areas to be at the ends due to loading at the ends. If by any chance the critical area is spotted at the middle of either Part 2 or Part 3, it can be bad. It is because, if the stresses are seen maximum at those areas where loading is not more correspondingly, this means that the stress distribution of that particular geometry is not proper and tend to fail soon. Both the stress

distribution images for Part 2 and Part 3 are shown below figures 7.1.3 and 7.1.4. The maximum stress found in Part 2 is 2.425 KSI which is equal to 16.71 MPa. The maximum stress found in Part 3 is 4.607 KSI which is equal to 31.76 MPa.

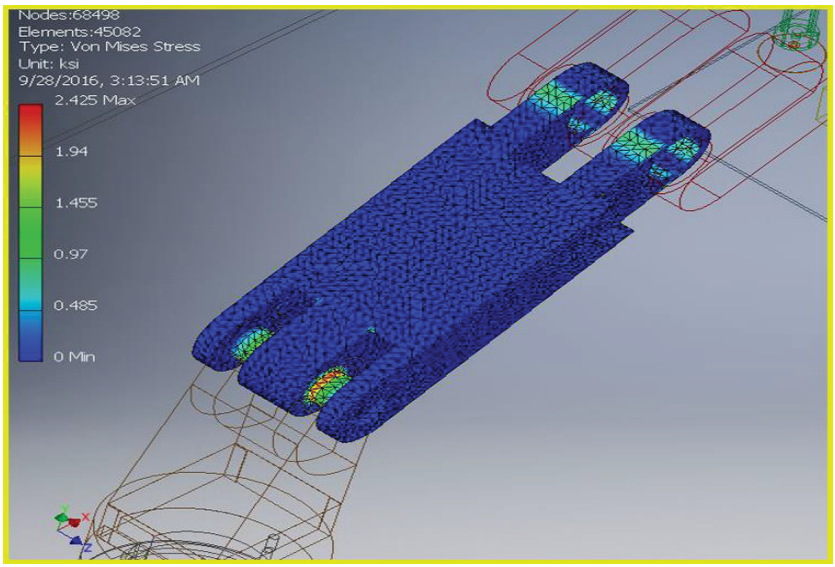

Figure 7.1.4: The Stress distribution of Part 2.

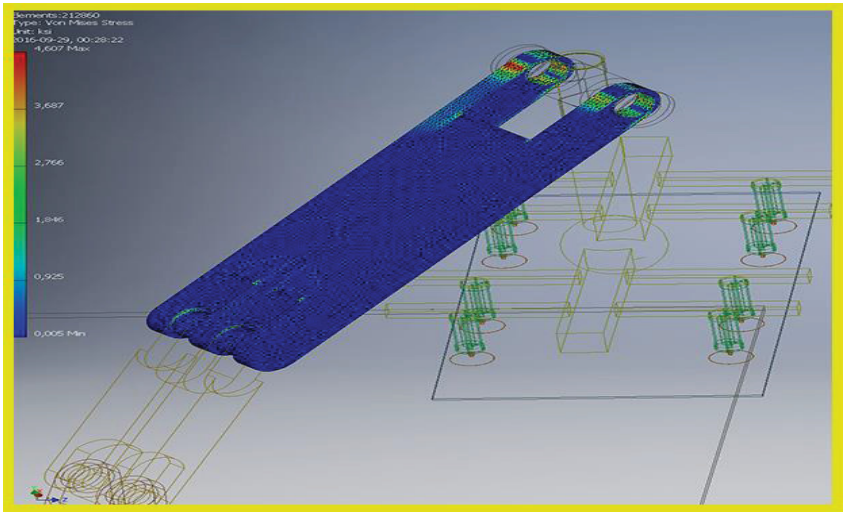

Figure 7.1.5: The Stress distribution of Part 3.

Part 4 and Part 5 both constitutes the end effector. Part 4 shown below figure 7.1.5 is a smaller part when compared to the size of remaining parts. It is suspended at the end of part 3 and rotates inside the holes on the right end of Part 3. It has 2 jobs to do. First one is to carry the weight if the end effector and move itself in correspondence with Part 2 and Part 3. The second job is to aid the rotation of end effector on its own axis. Naturally, as the load is acting on its center, the deformation is expected to be more at the center. The sides experience less deformation when compared to centers. The maximum stress on this part shown below figure 7.1.5 is found out to be 0.235 KSI which is equal to 1.67 MPa.

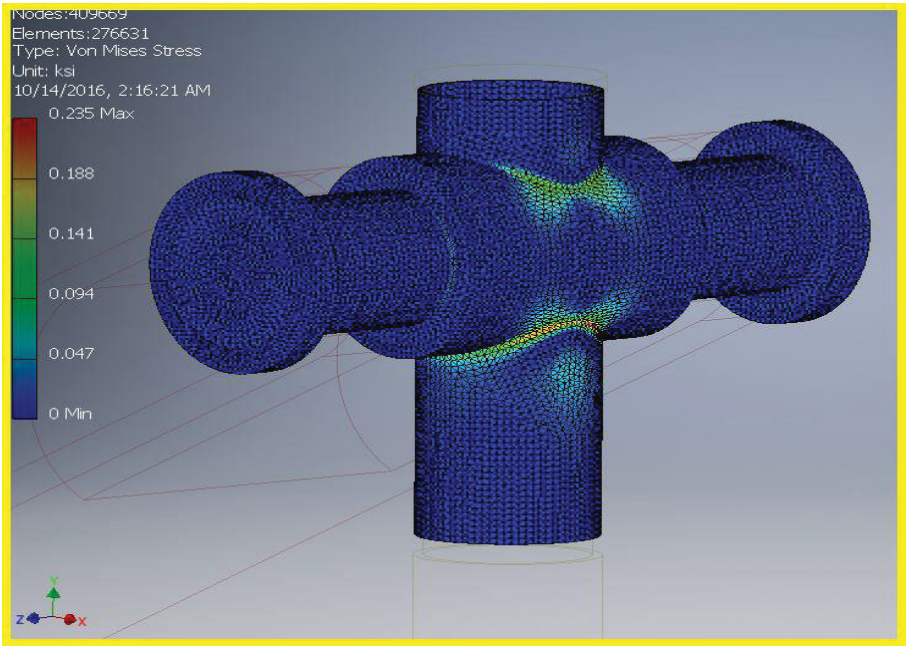

Figure 7.1.6: The Stress distribution of Part 4.

Part 5 is the backbone of end effector. The only duty it must hold the sheet. So, the maximum effect created by the pneumatic cylinders and the sheet is seen on this part. There are a lot of pretreated stresses in this part as we assume that the pneumatic cylinders are welded to this part (just to lock the DOFs of the cylinders). But those cylinders are assembled using screws and nuts. If observed clearly, we can see that the end effector is provided with the bases with holes and thread rods just for the cylinders to sit in. Due to the welded joints created on this part, the stress values that are generated by this simulation might be a bit more than the values. The stress distribution of part 5 is shown below figure 7.1.6. The maximum stress observed is 15.63 KSI which is equal to 107.13 MPa.

Now, we have the stress distribution data for all the 5 major parts here but to know whether these stresses are safe or not, we must check them. To perform this task, we take the help of the factor of safety concept. But before we get into this, the values of stresses shown along with these figures are at one particular time step. But, the whole process is for 7.5 seconds. They also

vary with the time and this point has already been explained along with Time vs Moment plot earlier in this section. To know where maximum and minimum stress occurs in the whole cycle, we take the help of Time vs Moment plots of all the parts and take out the maximum and minimum time steps in those plots. Those values are tabulated below in table 7.1.7.

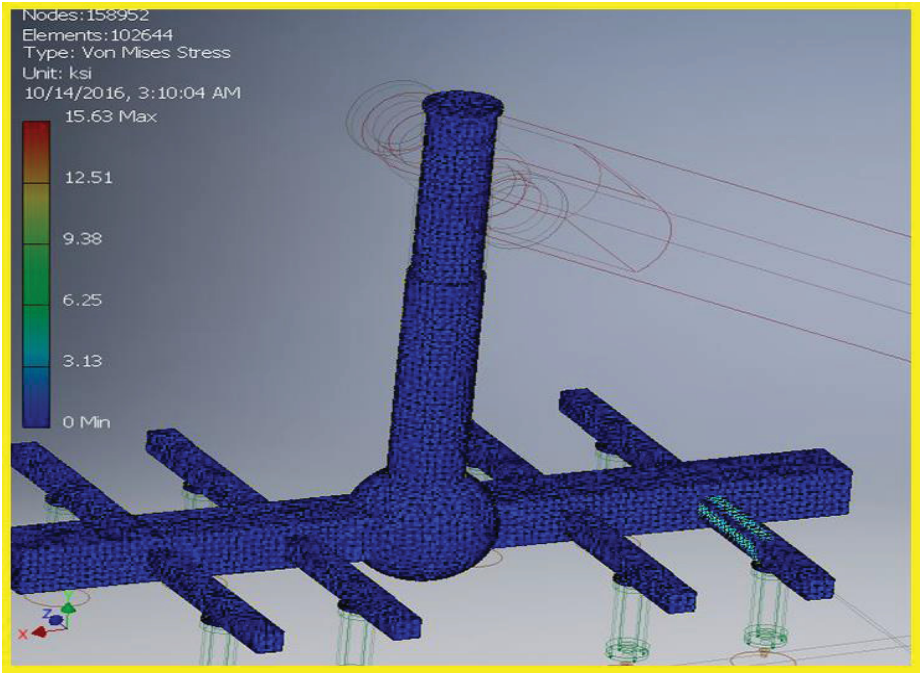

Figure 7.1.7: The Stress distribution of Part 5.

Table 7.1.1: The Table of maximum and minimum stresses.

PART	MAX. STRESS	TIME STEP AT WHICH MAX. STRESS OCCURS	MIN.STRESS	TIME STEP AT WHICH MIN. STRESS OCCURS
1	15.72 MPa	0.54 sec	14.14 MPa	0.136 sec
2	20.408 MPa	0.54 sec	4.52 MPa	0.136 sec
3	4.136 MPa	1.09 sec	1.31 MPa	0 sec
4	6.51 MPa	1.09	0.387 MPa	0 sec
5	15.92 MPa	1.22 sec	4.49 MPa	0 sec

The Factor of Safety is a term describing the load carrying capacity of a system beyond the expected or actual loads. Essentially, the factor of safety is how much stronger the system is than it usually needs to be for an intended load. Safety factors are often calculated using detailed analysis because comprehensive testing is impractical on many projects, such as bridges and buildings, but the structure's ability to carry load must be determined to a reasonable accuracy. Many systems are purposefully built much stronger than needed for normal usage to allow for emergency situations, unexpected loads, misuse, or degradation. Factor of safety is the ratio of Yield stress and Working stress. It gives a value which gives the load capacity of the part. If Factor of Safety is 1, this means the design can carry the load exactly that is required to carry. If the value is 2, this means it can carry twice the required load. Let us see the factor of safety values generated by Inventor for all the parts.

As we see that the Part 5 is not as strong as expected. The safety factor it has permits it only to carry the load of the sheet, which is good for this case but we expect the design to be stronger than this. There are many ways to make this stronger. We can either optimize it and redesign it accordingly or

can try a different material. The Part 5 is the end most part of the robotic arm. Part 5 showed less load bearing capacity with aluminum but, we have tried changing the material to CFRP (Carbon Fiber Reinforced Polymer). The reason for this is it is stronger and lighter material than aluminum. We cannot assign a material with more density. As density increases, weight increases and increase in weight of Part 5 might have bad effects on other arms. Our experiment worked and the part 5 has increased its capacity. The only problem with CFRP is it is relatively expensive. But again, selection of materials is a completely different study. We limit our study to the usage requirements of the industry.

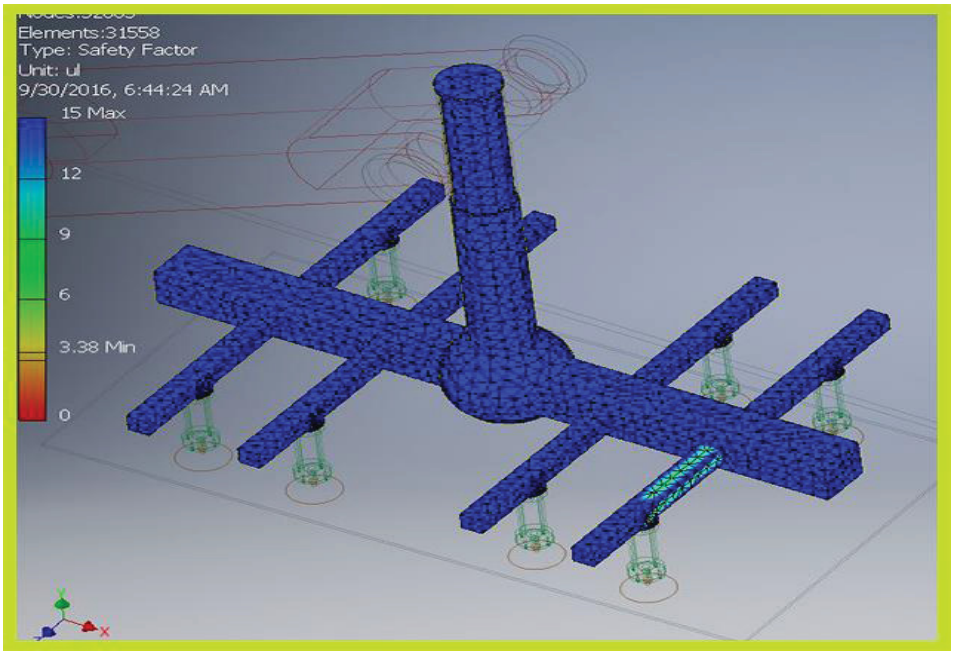

Figure 7.1.8: The FOS of Part 5.

These results that are seen are good at this instant. The model can take the weight of the sheet and if wanted, it can take more. But, this cannot be taken as the final word. The process in which the robotic arm is going to be used is a cyclic process. The same kind of loading is applied on the robotic arm repeatedly for a long period. We must also check for the approximate number

of cycles it can work before it fails. This leads us to the Fatigue Analysis of the Robotic arm.

7.2 Convergence

In the process of meshing the geometry and solving for the stress analysis, the stress results are needed to be found out more accurately. To achieve this, the geometry is meshed normally first and simulated. Then, the areas with more stress concentration is chosen and are meshed finely when compared to the previous mesh. Once the results are obtained, the areas with more stress concentration are meshed more finely. Here, for every step of the solution, the number of elements in the mesh increase. As mesh settings change, the results of a Stress Analysis may change and the accuracy of the stress results should be understood. Performing a convergence study refines the mesh and reduces the size of the elements, which will theoretically increase the accuracy of the next iteration of results. As mesh elements decrease in size but increase in quantity, the computational requirements to solve a given model increase. As mesh elements decrease in size, they reach a point of diminishing returns on the level of accuracy compared to the computational overhead and time required to compute the result. This means that a simulation requires more time to compute the results, but the result may change by an insignificant value. The solution is said to be converging if the stress value falls around same number as the number of time steps increases. The maximum stresses for part 2 are plot against the solution steps in the graph that is shown below. There is a significant increase in the number of elements for the increase of each solution step. The graph is plot using Matlab. The plot can be seen in figure 7.2.1. As seen in that plot, the stresses vary with increase in time steps (X-axis). As mentioned earlier, the number of mesh elements increases with time steps. That means, the peak most point in the curve has more number of meshed elements and therefore can be taken as the result closer to accuracy. As seen in the convergence plot, the last two stress values in the curve are very close to each other making the curve linear onwards. This is the proof that the solution converges and this stress value can be taken as the closest value to the stresses in reality. The values of stresses for each time step and the number of meshed elements for each time step are tabulated below in the table 7.2.1.

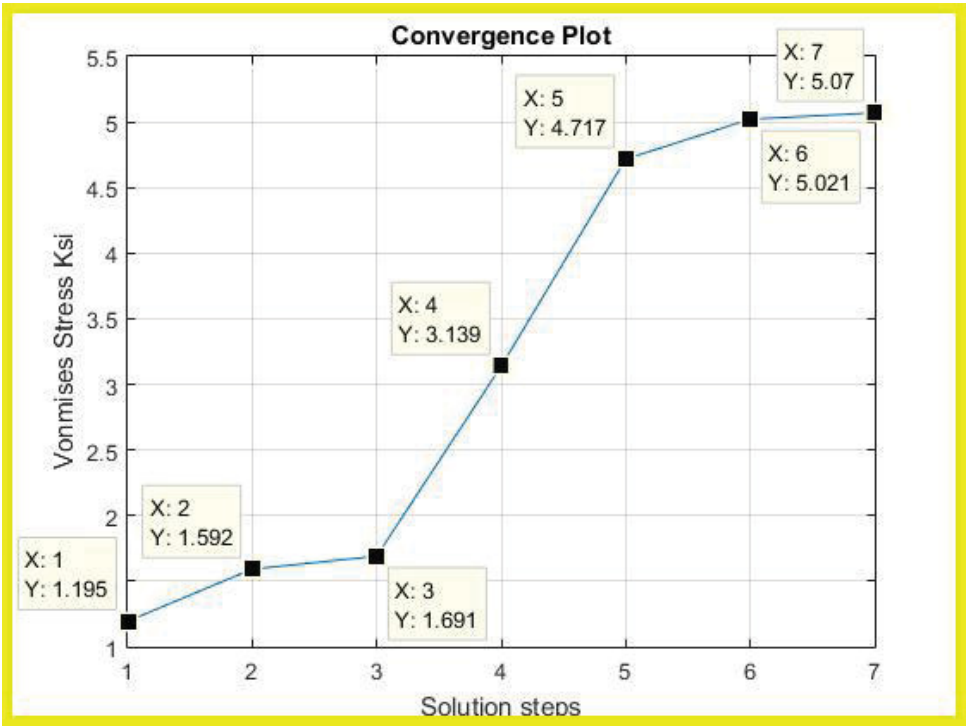

Figure 7.2.1: The Convergence Plot for Part 2.

Table 7.2.1: The Table of Number of Mesh Elements and Time Steps.

Time Steps	Number of Mesh Elements	Maximum Von Mises Stress KSI
1	1702	1.195
2	2051	1.592
3	4569	1.691
4	8988	3.139
5	22689	4.717
6	82850	5.07
7	271968	5.021

7.3 Fatigue Analysis

Fatigue is the weakening of a material caused by repeatedly applied loads. It is the progressive and localized structural damage that occurs when a material is subjected to cyclic loading. The nominal maximum stress values that cause such damage may be much less than the strength of the material typically quoted as the ultimate tensile stress limit, or the yield stress limit. When cyclic stresses are applied to a material, even though the stresses do not cause plastic deformation, the material may fail due to fatigue. Fatigue failure is typically modeled by decomposing cyclic stresses into mean and alternating components. Mean stress is the time average of the principal stress. The definition of alternating stress varies between different sources. It is either defined as the difference between the minimum and the maximum stress, or the difference between the mean and maximum stress. Engineers try to design mechanisms whose parts are subjected to a single type (bending, axial, or torsional) of cyclic stress because this more closely matches experiments used to characterize fatigue failure in different materials. For this, we need to have an approximate period where we will be able to assess that the material or design fails after these many number of cycles.

Fatigue failures are typically characterized as either low-cycle (1,000 cycles). The threshold value dividing low- and high-cycle fatigue is somewhat arbitrary, but is generally based on the raw materials behaviour at the microstructural level in response to the applied stresses. Lowcycle failures typically involve significant plastic deformation. Most metals with a body centered cubic crystal structure have a characteristic response to cyclic stresses. These materials have a threshold stress limit below which fatigue cracks will not initiate. This threshold stress value is often referred to as the endurance limit. In steels, the life associated with this behaviour is generally accepted to be $2x10^6$ cycles. In other words, if a given stress state does not induce a fatigue failure within the first $2x10^6$ cycles, future failure of the component is considered unlikely. For spring applications, a more realistic threshold life value would be $2x10^7$ cycles. Metals with a face center cubic crystal structure (e.g. aluminium, austenitic stainless steels, copper, etc.) do not typically have an endurance limit. For these materials, fatigue life continues to increase as stress levels decrease; however, a threshold limit is not typically reached below which infinite life can be expected. The behaviour of

these materials explained above can be exhibited with the help of S-N diagram, also known as a Wohler curve. This is a graph of the magnitude of a cyclic stress (S) against the logarithmic scale of cycles to failure (N). The progression of the S-N curve can be influenced by many factors such as corrosion, temperature, residual stresses, and the presence of notches. The Goodman-Line is a method used to estimate the influence of the mean stress on the fatigue strength[14]. Fatigue data on 6061-T6 aluminium were collected from the literature (Structural Alloys Handbook, 1989; Alcoa Structural Handbook, 1960 to construct a design fatigue curve. The low cycle data ($l0^3$ cycles) are all from axial strain controlled tests. Note that the data from the strain controlled tests fall right in with the rest of the data at greater than 10^3 cycles. Some of the high cycle data are from rotating beam tests. A fit to the 6061-T6 fatigue data was developed using the equation below.

$$S = \frac{E}{4\sqrt{N}} \ln\left(\frac{100}{100 - A}\right) + B$$

Where E = elastic modulus

N = Number of cycles to failure

S = Strain Amplitude times elastic modulus

and A and B are constants that are selected to make the equation fit the data. Note that S is treated like a stress based on the assumption of elastic behaviour. However, it does not represent a real stress when the elastic range is exceeded. As a first approximation, the fatigue properties can be estimated by taking A as the percentage reduction of area in a tensile test, RA, and B as the endurance limit Se. It should be noted that aluminium does not exhibit an endurance limit. The fit to the data is

$$S = \frac{14479}{\sqrt{N}} + 96.5 \text{ MPa}$$

The curve is shown with the available data from tests without any mean stress in Figure 7.3.1.

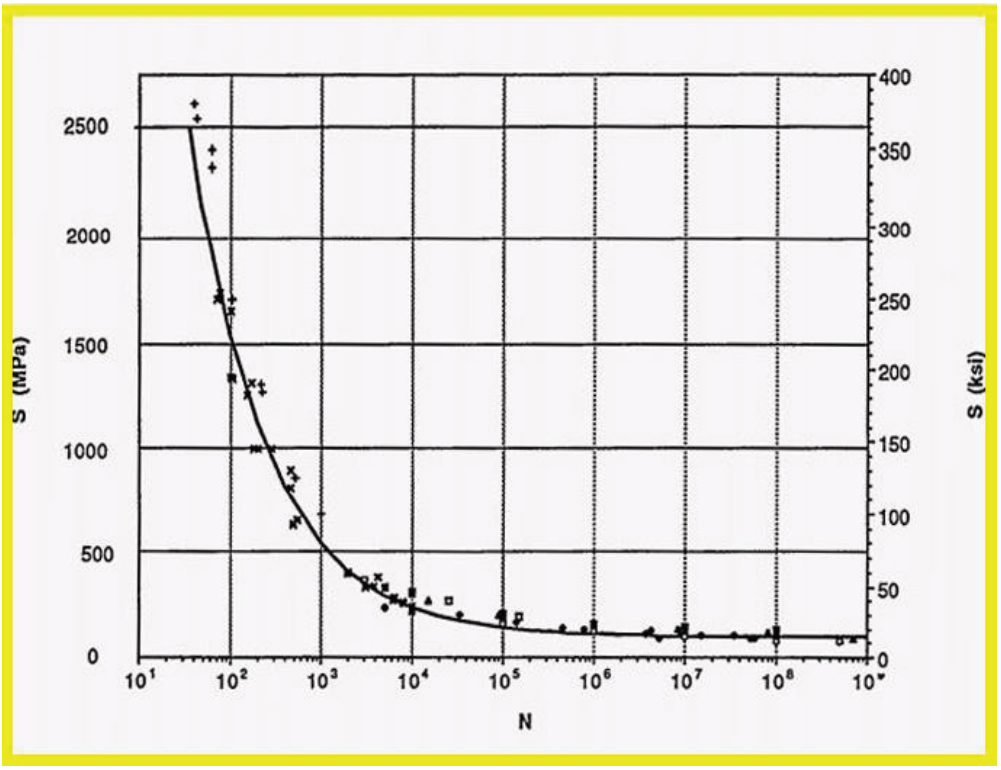

Figure 7.3.1: Aluminium 6061 Fatigue Data from Experiments **[15].**

Goodman relation is mathematically represented as

$$\frac{\sigma_a}{\sigma_e'} + \frac{\sigma_M}{\sigma_u} = 1$$

Where σ_a is alternating stress,

σ_M is mean stress,

σ_u is ultimate stress and

σ_e' is effective alternating stress.

Let us find the number of cycles to the failure one of the parts in the robotic arm, for example Part 2. From the table (7.1.1), we have

Maximum stress, σ_{min}= 4.521 MPa

σ_{max}= 20.408 MPa

From these values, we now have,

Stress range $\Delta\sigma = \sigma_{max} - \sigma_{min}$

alternating stress $\sigma_a = \frac{\Delta\sigma}{2}$

mean stress $\sigma_M = \frac{\sigma_{max}+\sigma_{min}}{2}$

The material used for this part is Aluminum. The data needed for the calculation of Number of Cycles is shown below.

The Ultimate tensile strength S_{ut} = 446 MPa

The Material Strength at 10^3 cycles $S_m = 0.95 \times S_{ut}$

Since the load acting on the part is bending load the constant value is taken as 0.95. If it is an axial loading, the constant value is taken as 0.75. Aluminum has no endurance limit. Some structural metals such as aluminum and copper, do not have a distinct limit and will eventually fail even from small stress amplitudes. In these cases, several cycles (usually 107) is chosen to represent the fatigue life of the material.

Endurance Limit for this part $S_e = K_a\, K_b\, K_c\, K_d\, K_e\, K_f\, S'_e$

Where S'_e is the experimental value of endurance limit R. R. Moore [16] experiment.

$$S'_e = 0.5 \times S_{ut}; \quad (S_{ut} \leq 1400\ MPa)$$

$$S'_e = 700\ MPa; \quad (S_{ut} > 1400\ MPa)$$

- K_a is the surface factor

$K_a = a(S_{ut})^b$ where a is the surface finish factor [17] which is 4.51

b is the exponent which is -0.265

K_a=0.023

- K_b is the size factor

$$K_b = -1.51 \times d^{-0.157};\ (51 < d \leq 254\ mm)\ [17]$$

d is generally referred to the diameter of the body. Since non-circular bodies have no particular diameter, we must calculate an effective diameter d_e to formulate the above equation. Considering our part as a rectangular part, the effective diameter is calculated as shown here.

$$d_e = 0.808 \times (h \times b)^{1/2}\ [17]$$

Where h = 0.153 mm and b = 0.08 mm

$K_b = 7.45 \times 10^{-4}$

- K_c is the Loading Factor

$$K_c = \begin{Bmatrix} 1 & bending \\ 0.85 & axial \\ 0.59 & torsion \end{Bmatrix}$$

- K_d is the Temperature factor

$$K_d = \frac{S_T}{S_{RT}}$$

Where S_T is the tensile stress at the T temperature and

S_{RT} is the tensile stress at the room temperature.

Since, our machine is placed at the working conditions in the room temperature, $K_d = 1$

- K_e is the Reliability Factor; $K_e = 1$

- K_f is the Miscellaneous-Effects Factor.

Though the factor K_f is intended to account for the reduction in endurance limit due to all other effects, it is intended as a reminder that these must be accounted for. The actual values of K_f are not available.

$$K_f = 1$$

Now, the endurance limit S_e = 3.825× 10^3 MPa

If we take S_n as the stress at n number of cycles, the equation to calculate S_n will be

$$S_n = A \times N^B$$

Where $A = 10^{(Log(S_m) - 3b)}$

$$B = \left(\frac{1}{Z}\right) \times \log\left(\frac{S_m}{S_e}\right)$$

$$Z = \log(N_1) - \log(N_2)$$

The boundary conditions for the materials without endurance limit (example Aluminum)

$S_n = S_m \; at \; N = N_1 = 10^3$

$S_n = S_f \; at \; N = \; N_2 = 5 \times 10^8$

Now, considering the Goodman equation,

$$\frac{\sigma_a}{\sigma_e'} + \frac{\sigma_M}{\sigma_u} = 1$$

$$\frac{\sigma_a}{\sigma_e'} = 1 - \frac{\sigma_M}{\sigma_u}$$

$$\sigma_e' = \left(\frac{\sigma_a}{\left(1 - \frac{\sigma_M}{\sigma_u}\right)} \right)$$

But we have another equation $\sigma_e' = S_n = A \times N^B$

$$N = \left(\frac{\sigma_e'}{A}\right)^{\frac{1}{b}}$$

Where N is the number of cycles which in case the calculation $4.3 \times (10^{17})$

7.4 Stress-Cycle (S-N Diagram)

In high-cycle fatigue situations, materials performance is commonly characterized by an S-N curve. This is a graph of the magnitude of an Alternating Stress Amplitude (σ_e') against the logarithmic scale of cycles to failure (N). We have plot them on the S-N diagram using the above data in Matlab. The plot obtained is shown below figure 7.3. Also the table 7.3.1 shows the number of cycles to failure for each part in the robotic arm.

Table 7.3.1: The Table of Number of Cycles to Failure for each part.

Part	Number of Cycles to Failure
1	5.8×10^{18}
2	4.3×10^{17}
3	3.1×10^{18}
4	1.29×10^{18}
5	6.28×10^{17}

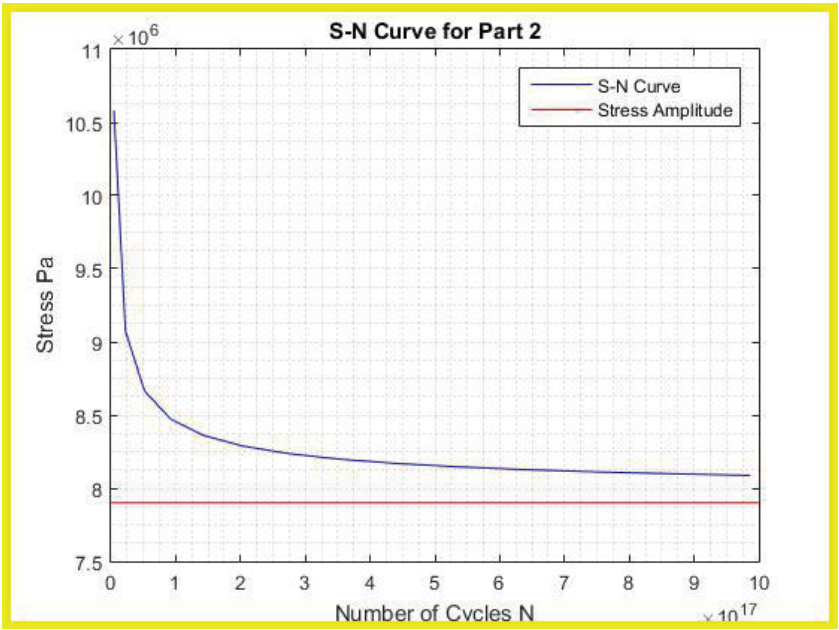

Figure 7.4.2: The graph between Time (sec) vs Stress (Mpa).

As seen, the plot above, the blue colored curve shows the stresses over the time. The red line is the line where we can see the stress amplitude or fatigue strength of the part which is calculated from the simulation. Theoretically speaking, the point where these 2 curves meet is the failure point of the material. But, as we can see that they do not meet, there is no scope of failure for this part theoretically. The life of the part ends before 10^3 cycles, it is the Low Cycle Fatigue. If it lasts till 10^8 cycles, it is the High Cycle Fatigue. If the part lasts or more than 10^8 cycles where the stress curve and endurance limit or fatigue strength become parallel to each other, then it has infinite life. This shows that this part is going to withstand for a good period of time.

8 Summary &Conclusions

8.1 Validation

For any design to be judged as a good design, it must be proven that it is useful for the purpose it is made for. In our case, we have analysed our model by creating the simulation environment which is mostly close to the actual working conditions and we have obtained some results. Now to check whether these results are satisfactory, we must take the Factor of Safety concept. Factor of safety is generally the ratio of Yield Stress of the design to the allowable stress. But Inventor has an option to set the ratio between Ultimate Tensile Stress to the allowable stress. A yield strength or yield point is the material property defined as the stress at which a material begins to deform plastically. Prior to the yield point the material will deform elastically and will return to its original shape when the applied stress is removed. Ultimate tensile strength is the capacity of a material or structure to withstand loads tending to elongate, as opposed to compressive strength, which withstands loads tending to reduce size. In other words, tensile strength resists tension (being pulled apart), whereas compressive strength resists compression (being pushed together). Ultimate tensile strength is measured by the maximum stress that a material can withstand while being stretched or pulled before breaking. If we observe the Stress-Strain curve, we can see that the Ultimate tensile strength always comes after the yield point. This point serves a very important observation.

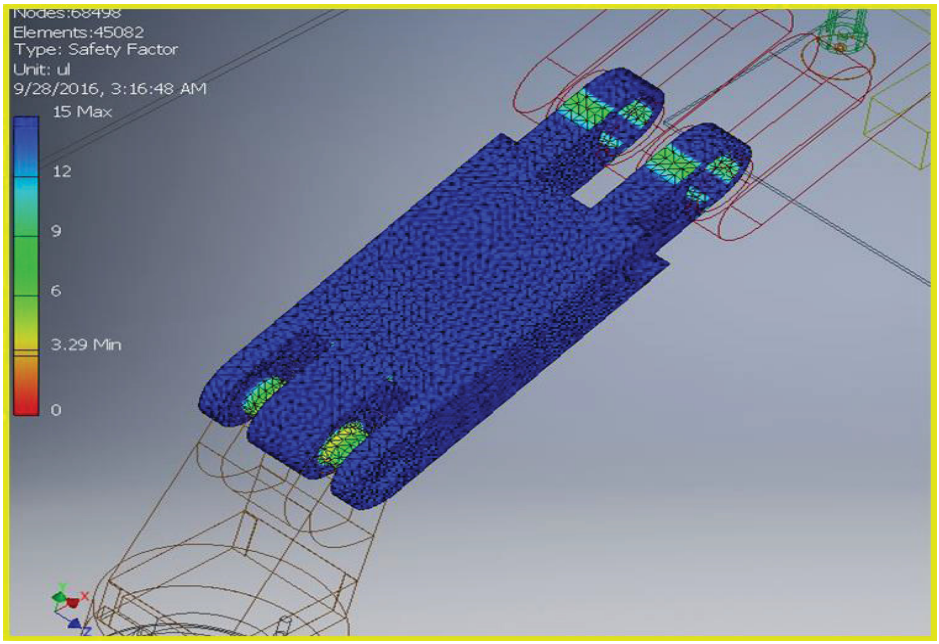

Figure 8.1.1: The Factor of Safety for Part 2.

If the Factor of safety of the parts in robotic arm is more than 3 when the ratio is yield stress to working stress, it will be much more than 3 if the ratio is Ultimate tensile strength to working stress. This means, the robotic arm far away from failure even its weight is increased by unavoidable accessories like servo motors, protective covers and probably a different and denser end effector. Our study shows that the robotic arm is not only strong enough for the required use but also strong enough to work for a long time without failure. Here, the factor of safety simulation figure 8.1 is shown above. All the parts of this robotic arm are having the minimum factor of safety more than 3 in those areas where the stresses are more. The table 8.1 below showing the factors of safety along with their stresses and materials assigned.

Table 8.1.1: The Table of Factors of Safety of all Parts

Part	Material	Minimum Safety Factor
1	Aluminium 6061, welded	3.89
2	Aluminium 6061, welded	3.29
3	Aluminium 6061, welded	3.5
4	Aluminium 6061, welded	3.1
5	CFRP	3.38

8.2 Conclusion

The main reason to make the choice of designing a robotic arm, firstly is the transport of the sheet from the stack to the shearing machine. Second, there is a space constraint we have in the industry. The stack of the sheets and the shearing machine are close to each other. They are so close that any other kind of transport such as a linear robot (conveyor) cannot be used. That leaves us with the only choice to build a robotic arm which can work in small and congested environments. The figure below shows the location and position of stack and shearing machine and we must design a robot arm that fits in this environment. As we observe the document, we can see that we have tested the robotic arm in all possible ways such as its load bearing capacity, motion ranges, joints etc. The motion demonstration of the robotic arm can be seen through the figures given in the appendix. The main task was to design a machine which fits in the environment and serves the purpose which has been achieved. But this is not the ultimate design. We tried to cover all the aspects of design and structural analysis in our work. But there is still a large chance of upgrading the machine.

As far as the current study is concerned, we are successful in determining the areas in which the stresses occur the most and able to show that those stresses are in limit also do not cause any considerable damage to the robot arm. The stress analysis that was performed was the non-linear stress analysis and all the geometric non-linearity is considered in the simulation. This shows that the stresses and deformation obtained are very close to the reality. The duration of the half cycle of the robotic arm in our simulation is 7.5 seconds, it means the sheet will be picked, transported and placed at its destination in 7.5 seconds which is a quick process This speed might not be compatible in the real-life use in the industry. We might have to slow down the process a bit. This 7.5 seconds' time limit isn't put out of blue. After many adjustments, trials, redesigns we have come to this time from 18 seconds to 7.5 seconds. Our motive to simulate it in such speed is that, if this machine can with stand motion loads in high speeds and still be safe, it can be a good machine at lower speeds. The speeds can always be adjusted by the user.

Figure 8.2.1: The position of Shearing Machine in Industry.

8.3 Future Works

Although a good effort is put in building and analysing this system, this cannot be taken for granted. There are many other parameters on which the quality of a model is dependent on. The easiest way to design and analyse a robotic arm is described and explained in this document. We cannot say it is perfect. In fact, no design is perfect. It is all about how close you can get to perfection. This model is needed to be optimized. We must have a detail explanation on what effect could take place on what area of the robotic arm if a parameter is changed especially design parameters like volume, thickness, material. Also, the cost study is needed to be performed in a more detail way. After all, a good machine is also judged on how affordable it can be.

There is always more room for innovation in any study. During this project, we came across many modern innovative automation techniques today's world has developed. If given a chance to do this project again, we are very much interested in applying those techniques. One such technique is application of fluidic muscles. A fluidic muscle is artificial version of human muscle. Not only this, many other techniques are applicable for this kind of machine. With all these additions, the machine gets upgraded into a super machine with ultimate application of automation.

References

[1] Minoru Baba, “Pick and Place for automatic test handler.” .

[2] Yang Liu and Michael Yu Yang, “Optimal Design of Remote Centre Compiance Devices of Rotational Symmetry.” .

[3] “Robot end effector,” Wikipedia, the free encyclopedia. 27-Jun-2016.

[4] M. M. B. S. Pachaiyyapan and T.Sridhar, “Design and Analysis of an Articulated Robotic Arm for various Industrial Applications,” 2015.

[5] FANUC America Corporation, Automated Bottle Pallet Unloader with FANUC Pick & Place Robot – Clear Automation. 2016.

[6] “Understanding Robot Specifications 101.” [Online]. Available: https://www.robots.com/blog/viewing/understanding-robot-specifications-101. [Accessed: 30-Sep-2016].

[7] “Inventor Forum.” .

[8] majentauk, Simulation Tips - Autodesk Inventor 2014. 2014.

[9] “Materials for Robot building an introduction.” .

[10] “Ashby charts.” Mike Ashby.

[11] “Aerospacs Specification Metals.” .

[12] Simulation Tips - Autodesk Inventor. .

[13] “Beam Boundary conditions.” .

[14] R. Stone, Fatigue Life Estimates using Goodman Diagrams. .

[15] Yahr, G.T., “36 Materials Science; Aluminium; Fatigue; Research Reactors; Presure Vessels; Welded Joints; Neutron Sources 360103; Mechanical Properties.” Office of Scientific and Technical Information, 01-Jun-1993.

[16] R.R. Moore, “Rotating Beam Fatigue Testing System.”

[17] K. N. R.Budnyas, Shigley’s Mechanical Engineering Design, Ninth. Shigley, 2003.

Appendix

Link to the Motion Demonstration of the Robotic Arm

https://www.youtube.com/watch?v=W3ImRT73SVk&feature=youtu.be

A. External Forces Acting on Parts

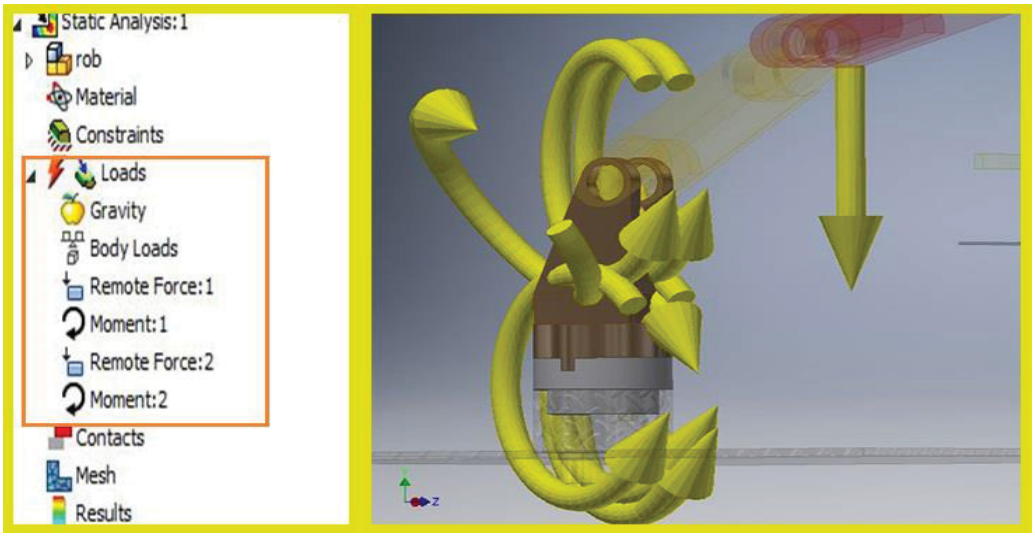

Figure A.1. The forces and moments of Part 1

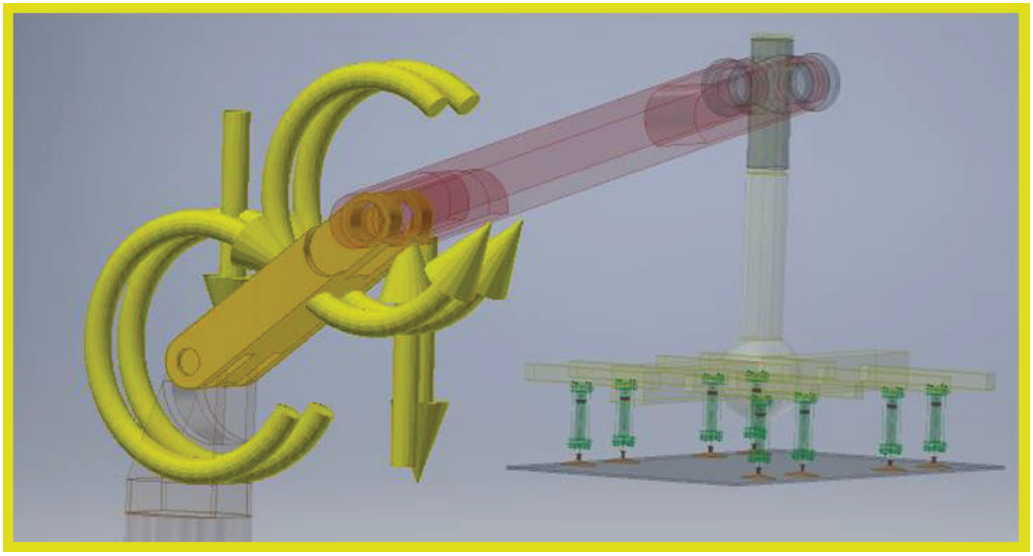

Figure A.2. The forces and moments of Part 2

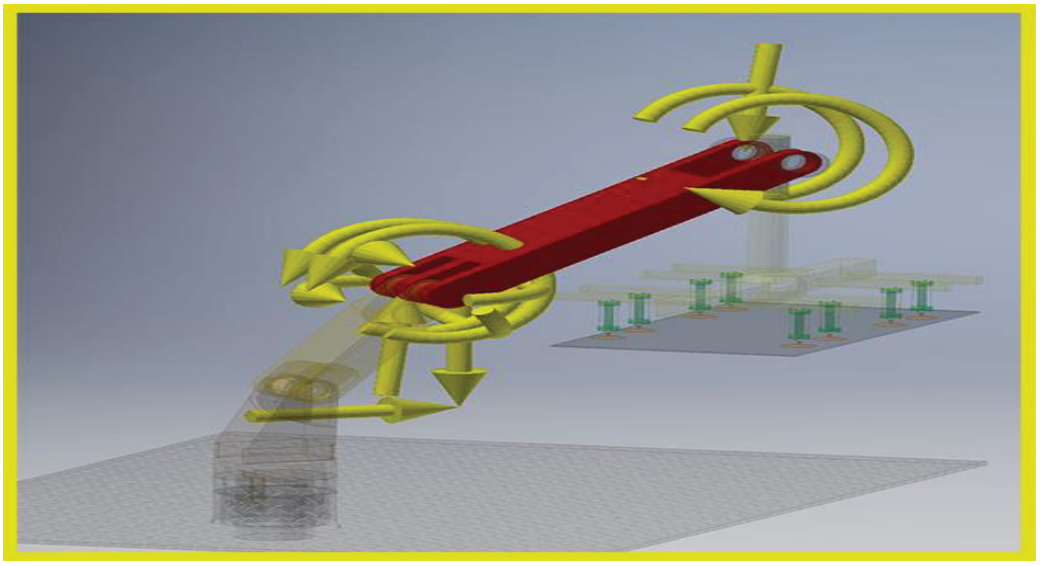

Figure A.3. The forces and moments of Part 3

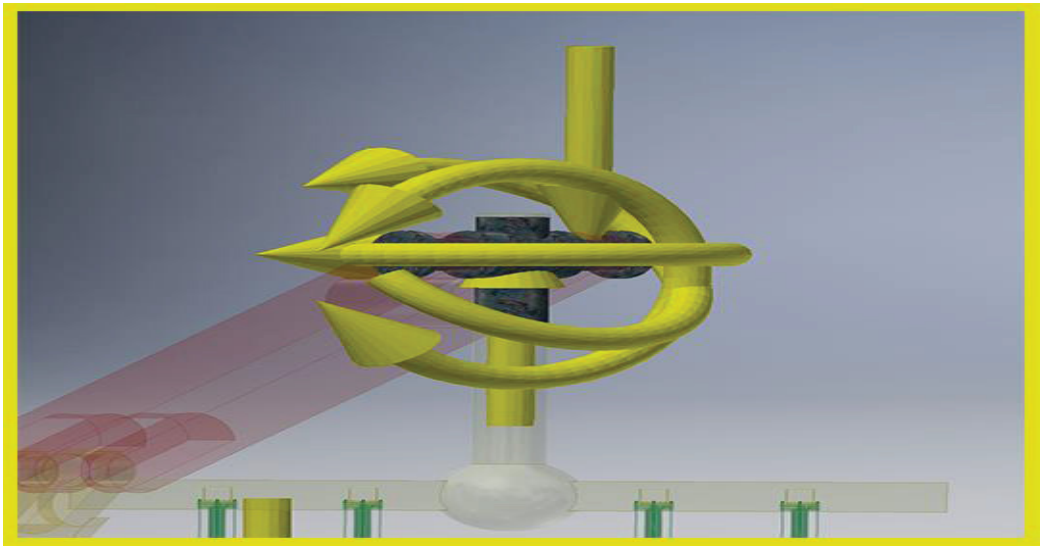

Figure A.4. The forces and moments of Part 4

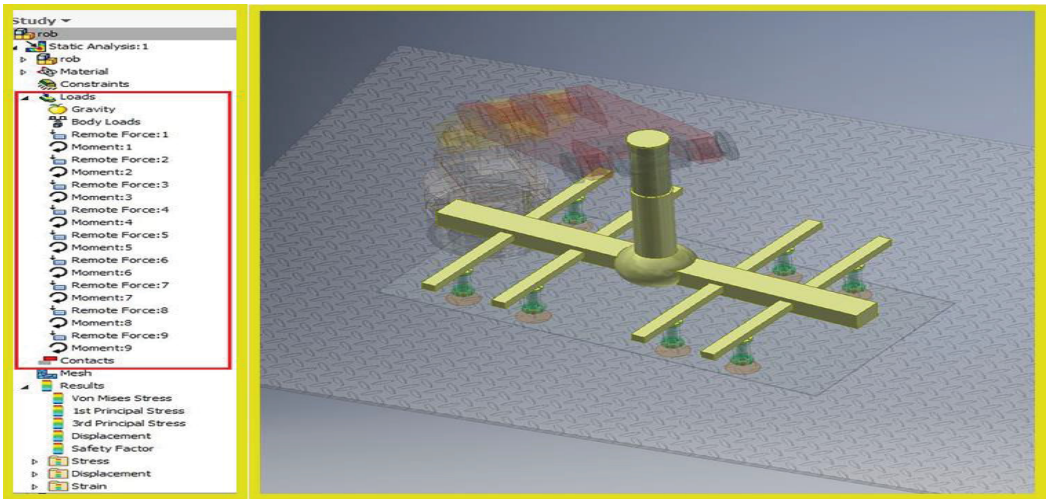

Figure A.5. The forces and moments of Part 5

B. Deformations on Parts

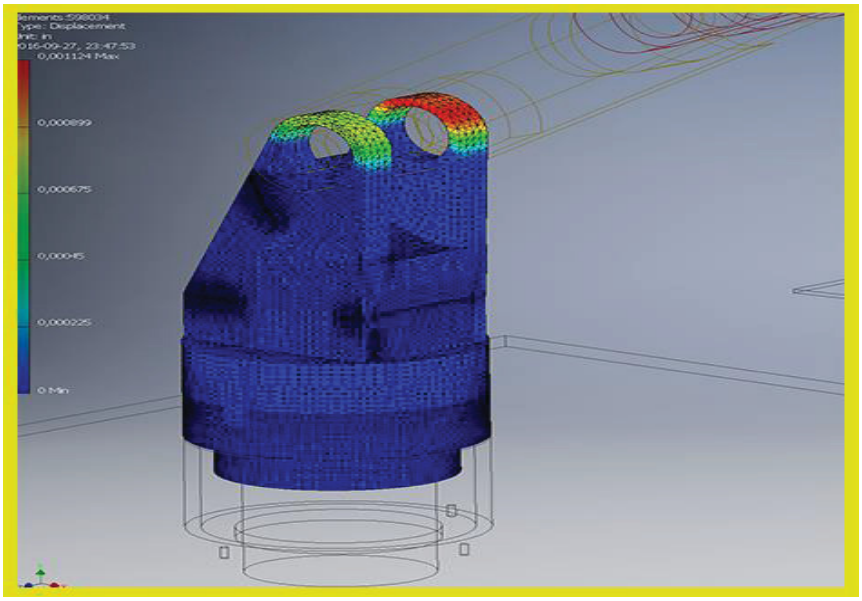

Figure B.1. The deformation of Part 1

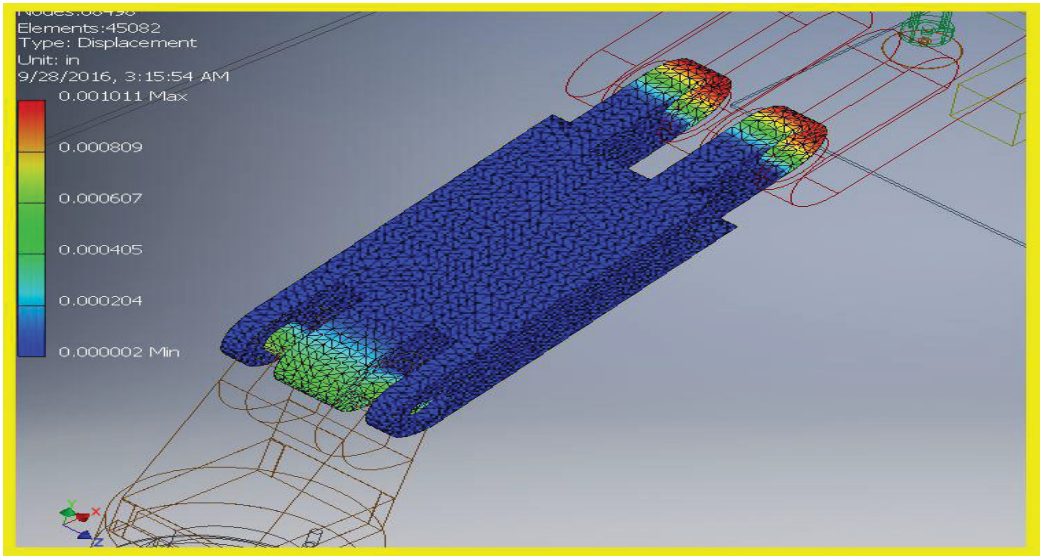

Figure B.2. The deformation of Part 2

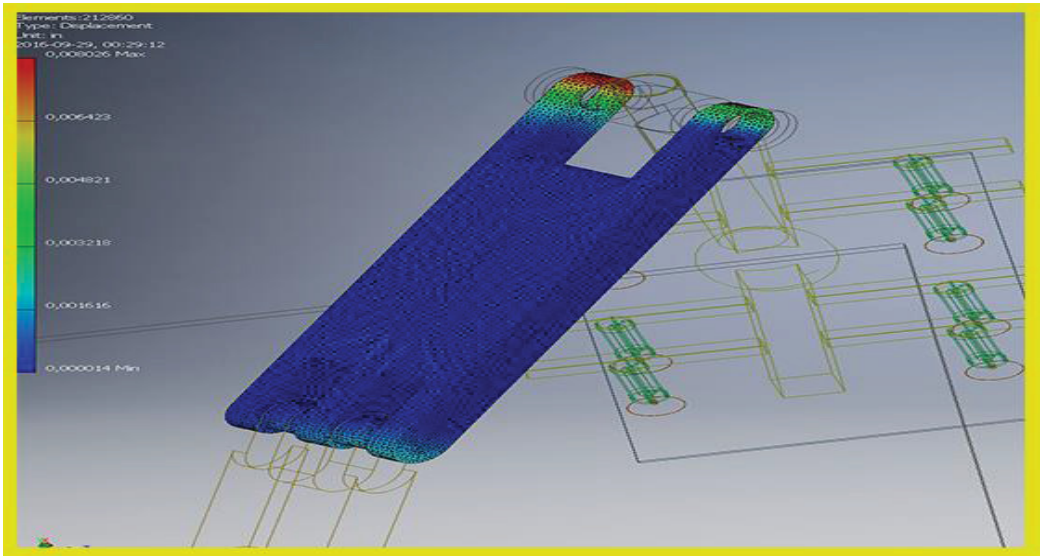

Figure B.3. The deformation of Part

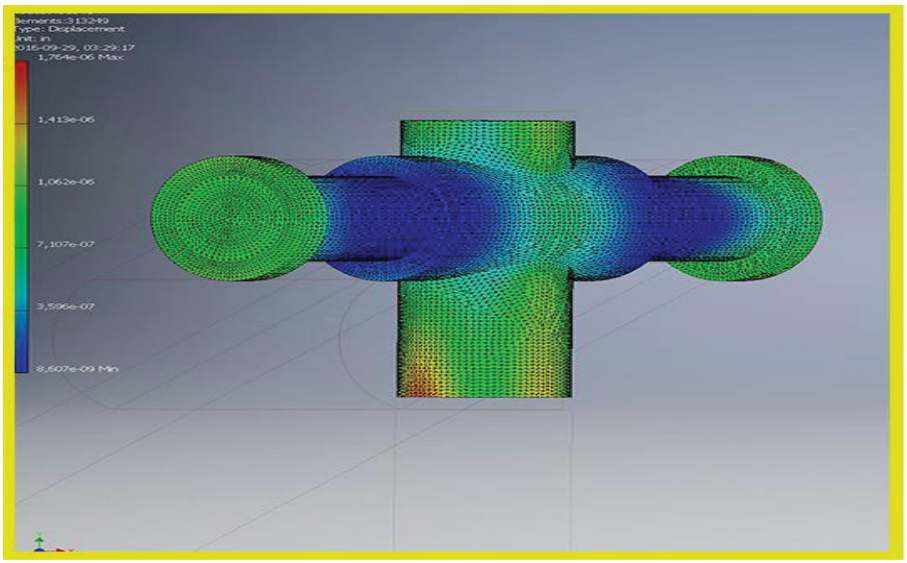

Figure B.4. The deformation of Part 4

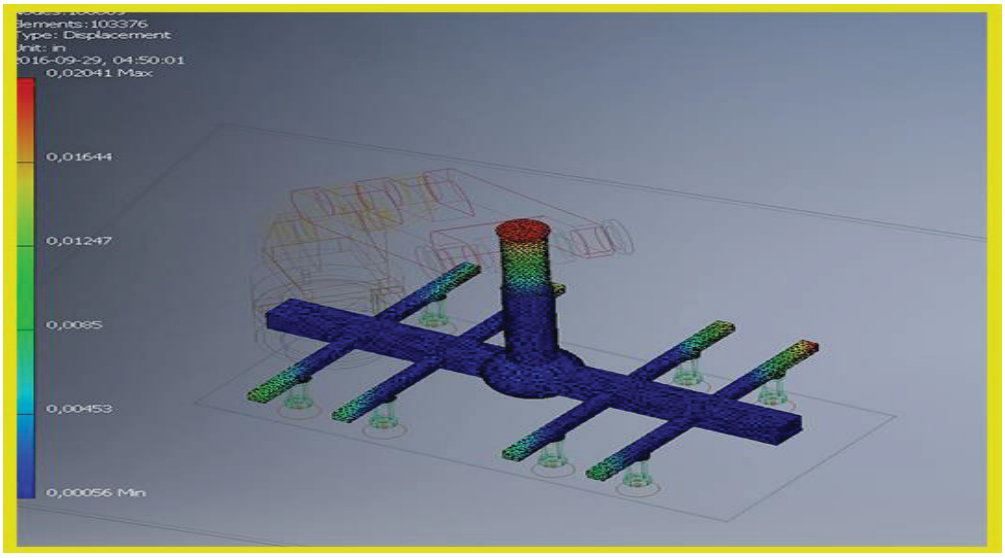

Figure B.5. The deformation of Part 5

C. Moment Vs Time Graphs

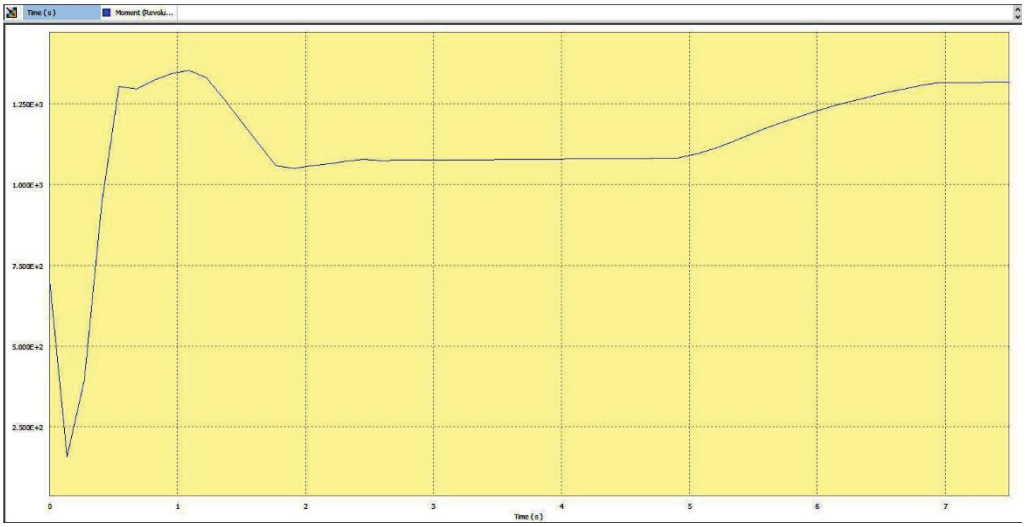

Graph C.1. The moment vs time plot for Part 2-3

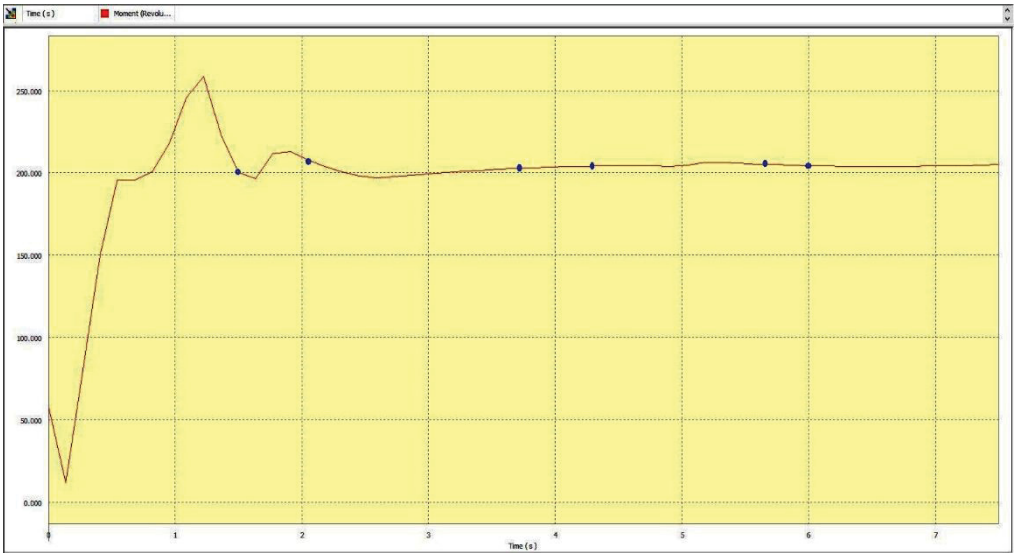

Graph C.2. The moment vs time plot for Part 3-4

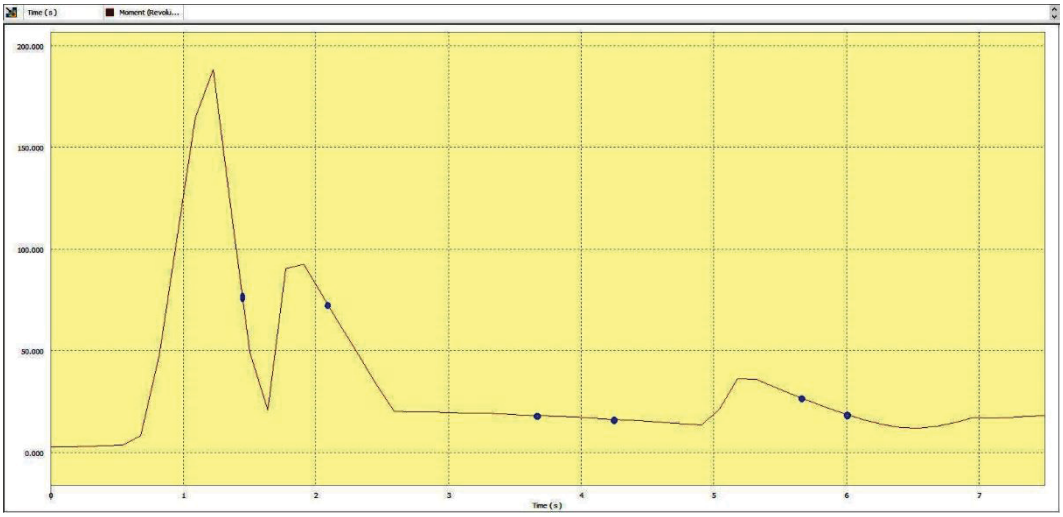

Graph C.3. The moment vs time plot of Part 4-5

D. The Factor of Safety on Parts

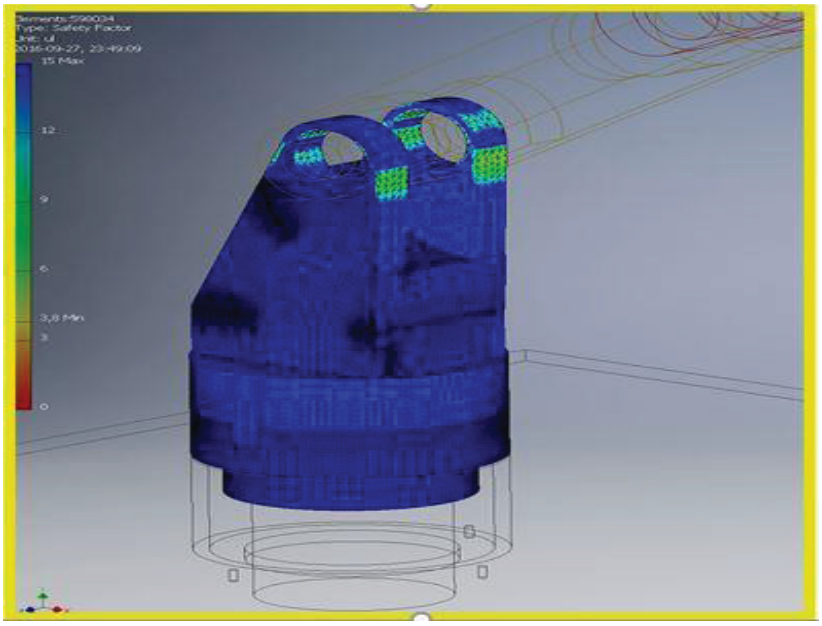

Figure D.1. The Factor of Safety of Part 1

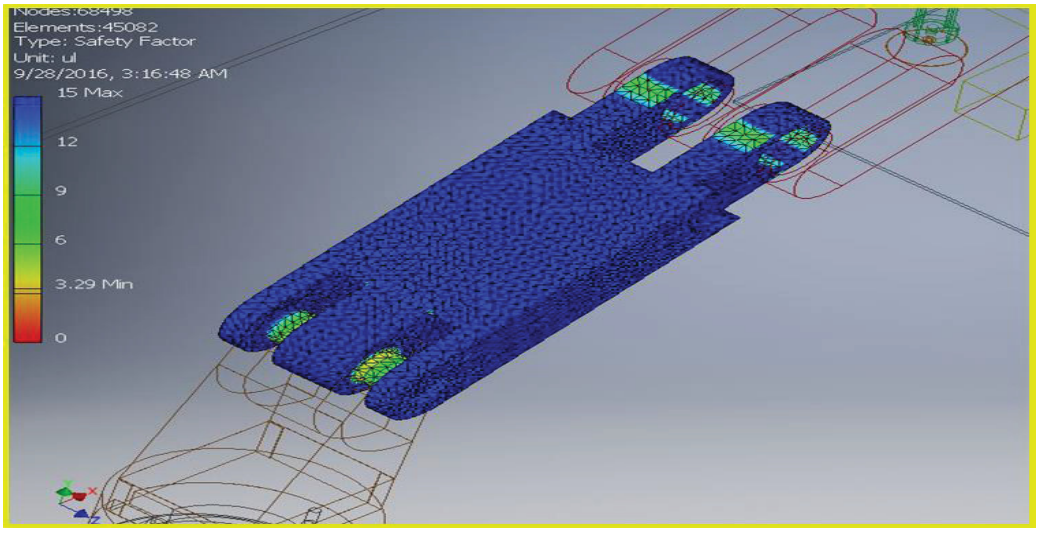

Figure D.2. The Factor of Safety of Part 2

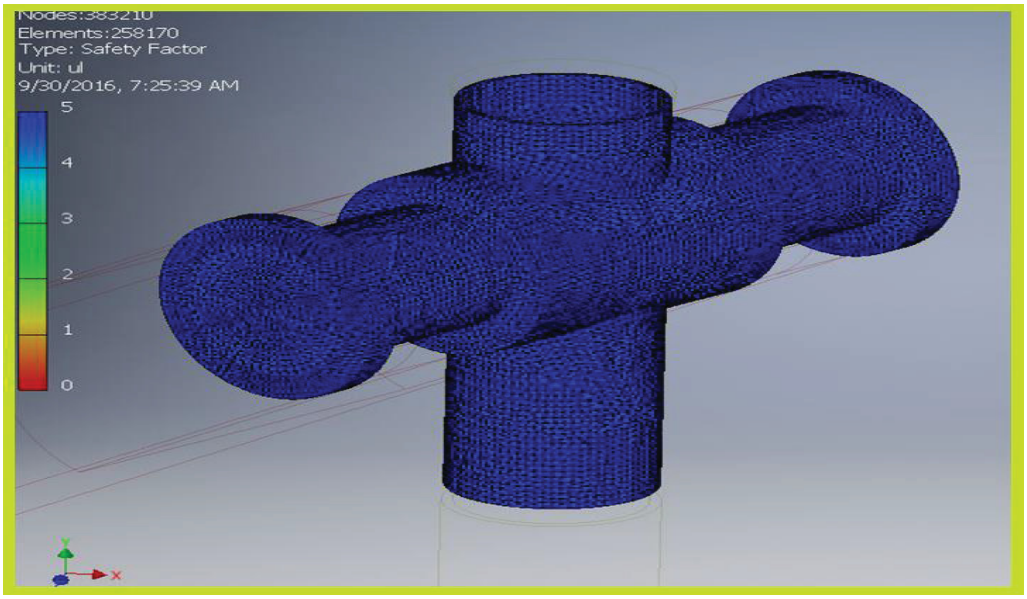

Figure D.3. The Factor of Safety of Part 4

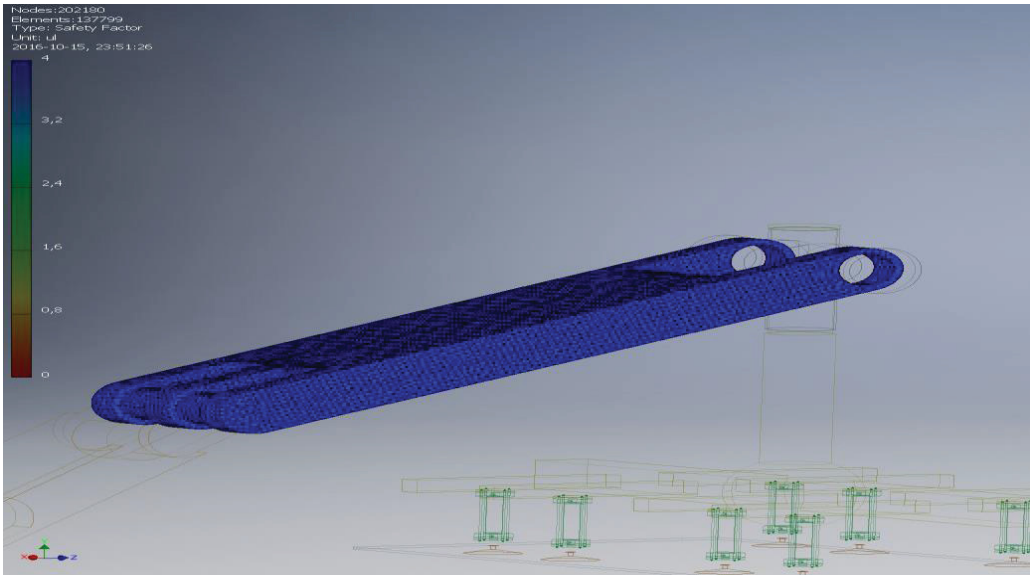

Figure D.4. The Factor of Safety of Part 3

E. Von-Misses Stress of Part 5 with CFRP material

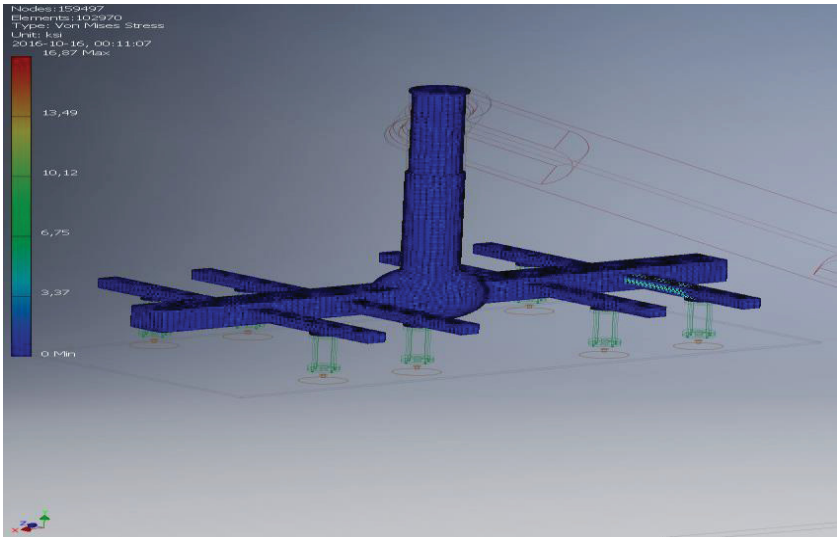

Figure E.1. The Von-Misses Stress of Part-5 with CFRP material

F. Matlab Code for calculating the Number of Cycles

```
Sut=446e+6; %Ultimate Tensile Stress
Sm=0.95*Sut; %Material Strength at 10^3 cycles
Se1=0.5*Sut; %Endurance Limit

h=153; %Height of the cross section-meters
br=80; %Breadth of the cross section-meters
de=0.808*((h*br)^0.5); %Effective Diameter
A=4.51;
Bb=-0.265;
Ka=A.*(Sut.^Bb); %Surface Factor
Kb=1.51*(de^(-0.157))*0.001; %Size Factor
Kc=1; %Loading Factor
Kd=1; %Temperature Factor
Ke=1; %Reliability Factor
Kf=1; %Miscellaneous Factor
Se=Ka*Kb*Kc*Kd*Ke*Kf*Se1;
N1=10e+3;
N2=5*(10e+8);
Z=log(N1)-log(N2);
b=(1/Z)*log(Sm/Se);
a=10^(log(Sm)-(3*b));

Smin=4.49e+6; %Minimum Stress in the cycle on the part
Smax=15.92e+6; %Maximum Stress in the cycle on the part
Srange=Smax-Smin; %Stress Range
Salter=Srange/2; %Alternating Stress
Smean=(Smax+Smin)/2; %Mean Stress
Syeild=296e+6; %Yeild Stress
P=Smean/Sut;
Q=(1-P);
Seffective=Salter/(Q); %Effective Alternating Stress at
Faliure
N=(Seffective/a)^(1/b); %Number Of Cycles for Failure

%Matlac code for S-N Curve
Sut=(50:50:650)*10^6; %Ultimate Tensile Stress
Sm=0.95*Sut; %Material Strength at 10^3 cycles
Se1=0.5*Sut; %Endurance Limit

h=153; %Height of the cross section-meters
br=80; %Breadth of the cross section-meters
de=0.808*((h*br)^0.5); %Effective Diameter
A=4.51;
```

```
Bb=-0.265;
Ka=A.*(Sut.^Bb); %Surface Factor
Kb=1.51*(de.^(-0.157))*0.001; %Size Factor
Kc=1; %Loading Factor
Kd=1; %Temperature Factor
Ke=1; %Reliability Factor
Kf=1; %Miscellaneous Factor
F=Ka.*Kb;
D=Kc*Kd*Ke*Kf*Se1;
Se=F.*D;

N1=10e+3;
N2=5*(10e+8);
Z=log(N1)-log(N2);
b=(1/Z)*log(Sm./Se);
a=10.^(log(Sm)-(3.*b));

Smin=4521580; %Minimum Stress in the cycle on the part
Smax=20408400; %Maximum Stress in the cycle on the part
Srange=Smax-Smin; %Stress Range
Salter=Srange/2; %Alternating Stress
Smean=(Smax+Smin)/2; %Mean Stress
Syeild=296e+6; %Yeild Stress
P=Smean./Sut;
Q=(1-P);
Qq=1./Q;
Seffective=Salter*Qq; %Effective Alternating Stress at Faliure
M=(Seffective./a);
B=1./b;
N=M.^(B); %Number Of Cycles for Failure
plot(N,Seffective,'b');
hold on
C=(0:1:9)*10e+16;
E=[7.9e+6 7.9e+6 7.9e+6 7.9e+6 7.9e+6 7.9e+6 7.9e+6 7.9e+6
7.9e+6 7.9e+6];
plot(C,E,'r');

xlabel('Time Sec');
ylabel('Stress MPa');
title('S-N Diagram');
legend('S-N Curve','Stress Amplitude');
title('S-N Curve for Part 2');
grid minor
```

School of Engineering, Department of Mechanical Engineering
Blekinge Institute of Technology
SE-371 79 Karlskrona, SWEDEN

Telephone: +46 455-38 50 00
E-mail: info@bth.se